NASA CONTRACTOR
REPORT

$T-70 \cdot 00858$

NASA CR-61320

LABORATORY DEVELOPMENT OF A SATELLITE EXPERIMENT FOR GAS-SURFACE INTERACTION STUDIES

By J. C. Zorn, G. R. Carignan, J. C. Pearl,
Denis P. Donnelly, and J. R. Caldwell

College of Engineering
University of Michigan
Dept. of Electrical Engineerir
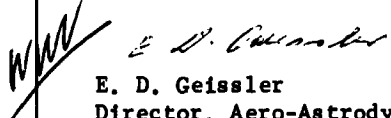Ann Arbor, Michigan

January 1970

Final Report

1. REPORT NO. CR-61320	2. GOVERNMENT ACCESSION NO.	3. RECIPIENT'S CATALOG NO.
4. TITLE AND SUBTITLE LABORATORY DEVELOPMENT OF A SATELLITE EXPERIMENT FOR GAS-SURFACE INTERACTION STUDIES		5. REPORT DATE January 1970
		6. PERFORMING ORGANIZATION CODE
7. AUTHOR(S) J. C. Zorn, G. R. Carignan, J. C. Pearl, Denis P. Donnelly, and J. R. Caldwell		8. PERFORMING ORGANIZATION REPORT #
9. PERFORMING ORGANIZATION NAME AND ADDRESS College of Engineering University of Michigan Dept. of Electrical Engineering Ann Arbor, Michigan		10. WORK UNIT NO.
		11. CONTRACT OR GRANT NO. NAS8-21450
		13. TYPE OF REPORT & PERIOD COVERED
12. SPONSORING AGENCY NAME AND ADDRESS Aero-Astrodynamics Laboratory George C. Marshall Space Flight Center Marshall Space Flight Center, Alabama 35812		Contractor Report
		14. SPONSORING AGENCY CODE

15. SUPPLEMENTARY NOTES This work was performed with Gary R. Swenson as contract monitor.

16. ABSTRACT

During 1966 and 1967 under research contract with the George C. Marshall Space Flight Center (Contract NAS8-21096), the Molecular Beam Laboratory and the Space Physics Research Laboratory of the University of Michigan defined an experimental concept for making quantitative measurements of important physical properties of gas-surface interactions.

The objective of this study has been to develop a technique and associated flight hardware for measuring the velocity distribution of molecules in a rarefied gas; the resulting experiment package is to be used for the measurements of gas-surface inter-action phenomena in situ in the earth's atmosphere.

The metastable time-of-flight system described in this report has been prepared to achieve this objective. Specifically, it has been demonstrated that (a) the velocity distributions of metastable atoms produced by electron impact can be measured with a time-of-flight analyzer, and (b) these distributions can be related to the incident gas flux through kinematic considerations. In addition, breadboard electronics for data analysis in flight experiments has been successfully tested in the laboratory. Thus, the basis for the measurement has been established.

Distribution of this report is provided in the interest of information exchange. Responsibility for the contents resides in the author or organization that prepared it.

17. KEY WORDS	18. DISTRIBUTION STATEMENT CATEGORIES 13 and 14 E. D. Geissler Director, Aero-Astrodynamics Laboratory

19. SECURITY CLASSIF. (of this report) UNCLASSIFIED	20. SECURITY CLASSIF. (of this page) UNCLASSIFIED	21. NO. OF PAGES 103	22. PRICE

MSFC - Form 3292 (May 1969)

PRECEDING PAGE BLANK NOT FILMED.

TABLE OF CONTENTS

TABLE OF CONTENTS (Continued)

TABLE OF CONTENTS (Concluded)

ACKNOWLEDGMENTS

PROJECT PERSONNEL

Barrett, John   Assistant Research Physicist

Caldwell, John R.   Research Associate

Carignan, George R.   Director,
                               Space Physics Research Laboratory

Donnelly, Denis   Lecturer in Physics

Heppner, Richard   Assistant Research Physicist

Kaslow, David E.   Assistant Research Physicist

Konrad, Gerhard   Consultant*

Lipp, Barbara   Secretary

Lockhart, James   Assistant Research Physicist

O'Bara, Kenneth   Assistant in Research

Pearl, John C.   Assistant Research Physicist

Pichlik, Russell   Assistant Research Physicist

Shaw, Ralf   Technician

Zorn, Jens C.   Associate Professor of Physics

*Now at the MIT Lincoln Laboratory

LIST OF ILLUSTRATIONS

LIST OF ILLUSTRATIONS (Continued)

LIST OF ILLUSTRATIONS (Concluded)

1. INTRODUCTION

1.1 BACKGROUND OF PRESENT RESEARCH

During 1966 and 1967 under research contract with the George C. Marshall Space Flight Center (Contract NAS8-21096) the Molecular Beam Laboratory and the Space Physics Research Laboratory of the University of Michigan defined an experimental concept for making quantitative measurements of important physical properties of gas-surface interactions. This research pointed the way to the definition of a feasible satellite experiment to make gas surface interaction measurements in situ in the earth's atmosphere. The final report of this research served as a basis for a proposal for additional effort to further study the suggested technique and to move toward the final design of a satellite experiment. This additional research was funded under Contract NAS8-21450, and the results are reported herein.

Essentially all of the planned objectives of this latter study were realized. Operation of the experiment in the laboratory has successfully demonstrated the collimation technique and has shown conclusively that the velocity distribution in a metastable beam can be accurately measured. A flight-type electron gun assembly and a breadboard data processing sub-system were designed, constructed and tested.

The essential features of a flight experiment are now understood. The current status of the experiment is summarized in the closing section of this report, and a program for flight application is suggested.

1

1.2 PROPOSED EXPERIMENTAL CONFIGURATION

1.2.1 General Description

The objective of the proposed experiment is to explore the interactions of nitrogen molecules with surfaces under conditions of relative velocity and general environment found on an earth satellite. The velocity of the N_2 molecules relative to the satellite before impact is relatively uniform and is on the order of 10^6 cm/sec; their velocity distribution after scattering from test surfaces is to be measured. For the experiments as currently conceived, the maximum altitude at which useful measurements can be performed ($\approx$350 km) is reached when the reflected flux of N_2 is too weak to be detected, while the lowest operational altitude (about 100 km) is that at which the mean free path of slow molecules within the instrument is appreciably less that the characteristic dimensions of the detector.

The general features of the experiment are shown in Figure 1.1. An enclosed analyzer is used to measure the angular distribution and velocity distribution of the nitrogen flux which is reflected from a target surface. Molecules strike the target surface at an angle determined by the attitude of the satellite with respect to its velocity vector. Those molecules which are reflected from the surface within a narrow range of angles enter the time-of-flight analyzer; the readout from the analyzer enables one to deduce the velocity distribution of the reflected molecules. Noteworthy features of the proposed experiment are that no moving parts are employed other than the target surface indexer, and that target surfaces are

TARGET SURFACES
ON INDEXING
SHAFT

10^{14} MOLECULES
$CM^{-2}SEC^{-1}$

ELECTRON
GUN

~10^{-2} LOSS IN REFLECTION

~10^{-3} DUTY CYCLE

~10^{-5} FOR $\sigma(e + N_2 \rightarrow N_2^* + e)$
(10^{-8} LOSS IN EXCITATION)

PULSED
ELECTRON
BEAM

COLLIMATOR

~20 CM

AUGER
SURFACE

~10^{-1} FOR
AUGER DETECTION
EFFICIENCY

CHANNELTRON

~10^3 PULSES/SEC
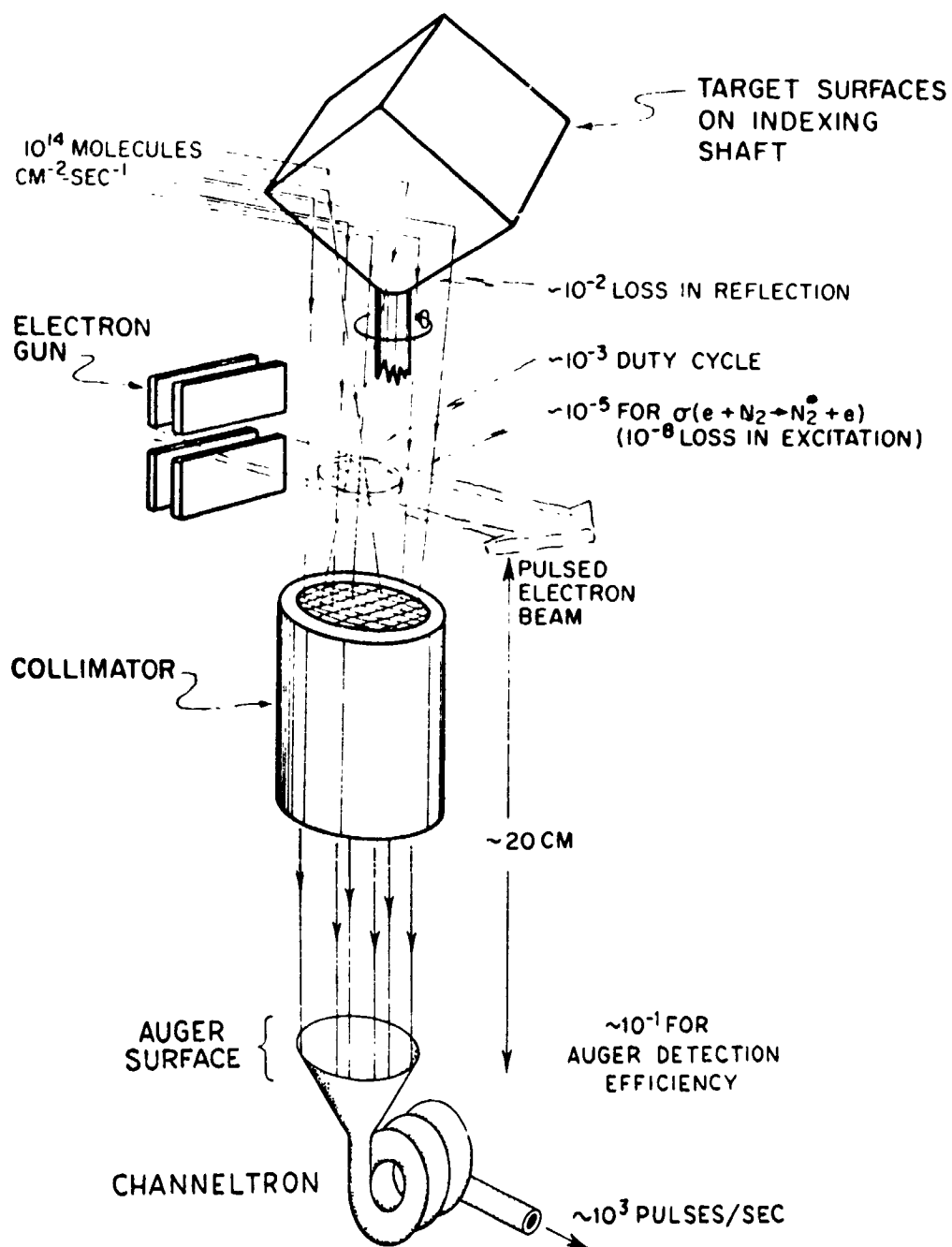
Figure 1.1 N_2 time-of-flight analyzer operation.

3

directly exposed to the space environment.

1.2.2 Measurement of Velocity Distributions in Neutral Gases

The velocity distribution of a beam of <u>ions</u> inside an
apparatus is governed more by electric fields within the
enclosure than by the velocities of the incoming neutral
molecules. This suggests that velocity analysis on the reflected
flux should be done on the molecules while they are electrically
neutral. One possible way of performing such an analysis
would be to use a rotating mechanical velocity filter. However,
the maximum molecular velocity for which these filters can
operate is less than 10^6 cm/sec and, in addition, the requirement
of operating the filter at high rotational velocities makes it
unsuitable for flight experiments. Consequently, we propose
to use a periodically pulsed electron beam to create a spatially
concentrated group of neutral, metastable N_2 molecules; the
time of flight of these metastables over a 20 cm path in the
apparatus will be observed. Since the metastable molecules
are neutral, the detector output will provide an accurate
measure of the velocity distribution of the reflected neutral
flux. No moving mechanical parts are involved, and electron
guns which give short pulses can be constructed with ease, so
the system is well suited for analysis of very fast molecular
beams.

The operation of the N_2 TOF analyzer is most easily des-
cribed with reference to Figure 1.1. The molecules enter the
analyzer after reflection from a target as shown in the figure.
The molecules pass into a pulsed electron gun where some of them

4

are excited to their metastable state. If a metastable
molecule passes through the collimator (an array of parallel
tubes) without collision, it will arrive in its excited state
at the cathode of a windowless electron multiplier. Here the
deexcitation of the metastable molecule causes the ejection of
an electron (Kaminsky, 1965), giving an output pulse. The output
of the multiplier is therefore a series of pulses at a rate
proportional to the flux of metastable molecules through
the analyzer.

The use of a cluster of TOF analyzers to measure reflected
N_2 at five different angles is shown in Figure 1.2. Note
that one electron gun serves for all five units. The pulse
of electrons which excites the metastable N_2 will also excite
optical levels of the molecules; photons from the decay of
these short-lived levels will arrive at the Auger surface
within nanoseconds of the electron pulse time, and the detector
signal which comes from these photons can be used to calibrate
the zero-time of the TOF analyzer.

1.2.3 Rejection of Background N_2

The metastable time-of-flight analyzer is well adapted
to discriminating against background molecules because it
measures both the direction and the speed of the incoming
particles. As discussed more fully in Section 4 of this
report, by collimating the metastable beam the instrument
registers only molecules which enter the electron bombardment
region with their momenta in a direction nearly parallel to
the collimator axis. Consequently, by orienting the collimator
to face the target surface under investigation, essentially
all metastable molecules which strike the Auger detector will

5
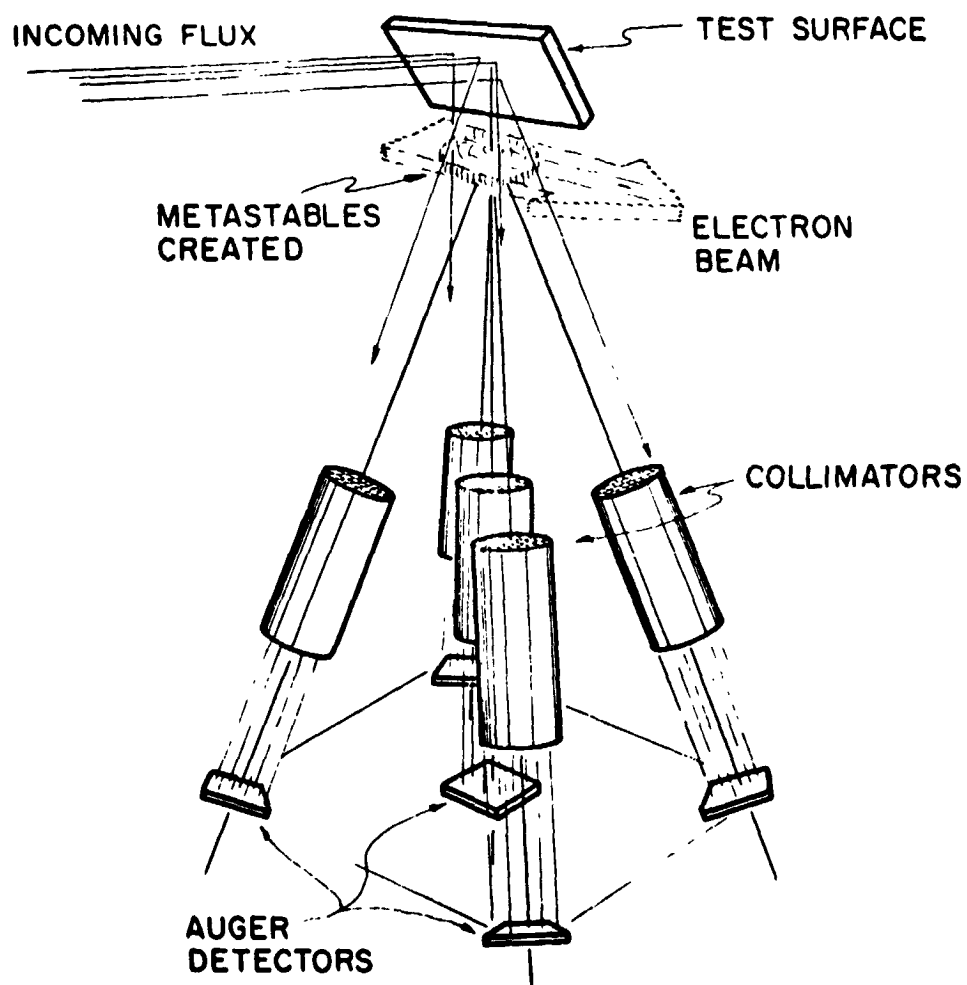
Figure 1.2 Analyzer cluster for angular distribution measurements of reflected metastable N_2.

have come from that surface.

Because the electron excitation process produces only a small change in the velocity of the incoming molecules, the TOF analysis accurately measures the distribution of speeds of the particles arriving from the target surface. As a result, the high speed ($>5 \times 10^4$ cm/sec) component of the reflected flux should be relatively free of background because the molecules which strike the target after previous collisions with the instrument will be very nearly thermalized and therefore contribute only to the low speed portion of the data.

2. EFFECT OF RECOIL ON THE VELOCITY DISTRIBUTION OF METASTABLE MOLECULES PRODUCED BY ELECTRON IMPACT

2.1 INTRODUCTION

Since the object of the satellite experiment is to investigate gas-surface interactions, it is necessary to know accurately the velocity distributions in both the incident and reflected gas beams. Thus, it is imperative to understand any systematic effects introduced by the MTOF analyzer itself.

The effects of using an electron pulse of finite duration, of a finite electron-gas beam interaction region, and of velocity dependent scattering from the beam (see Appendix II) have been discussed in an earlier report on this experiment (Zorn and Pearl, 1967). The effect of a finite lifetime of a metastable state is investigated in Section 3 of the present study. The principal remaining systematic effect, the influence of recoil from electron impact on the velocity distribution, is discussed in this section (see also Pearl, et al., 1969).

In order to investigate recoil effects experimentally, a collimated beam of helium gas was directed into a laboratory version of the MTOF analyzer. Helium was chosen as the test gas because its low mass and large excitation energy lead to highly exaggerated distortions of the metastable velocity distribution; a situation in which recoil effects are large was desired in order to facilitate comparison between theory and experiment.

Geometrical parameters for the present experiment are indicated in Figure 2.1. Time-of-flight spectra were taken at various electron energies and outgoing beam angles; the incoming

TO PULSER

TO TOF ANALYSIS

DETECTOR

PRE-AMP

0.5 mm

$L = 28.6$ cm

$\pi - \Phi$

θ

1.6 mm

2.0 mm

GAS SOURCE

5.9 cm

14.6 cm

PULSED ELECTRON GUN
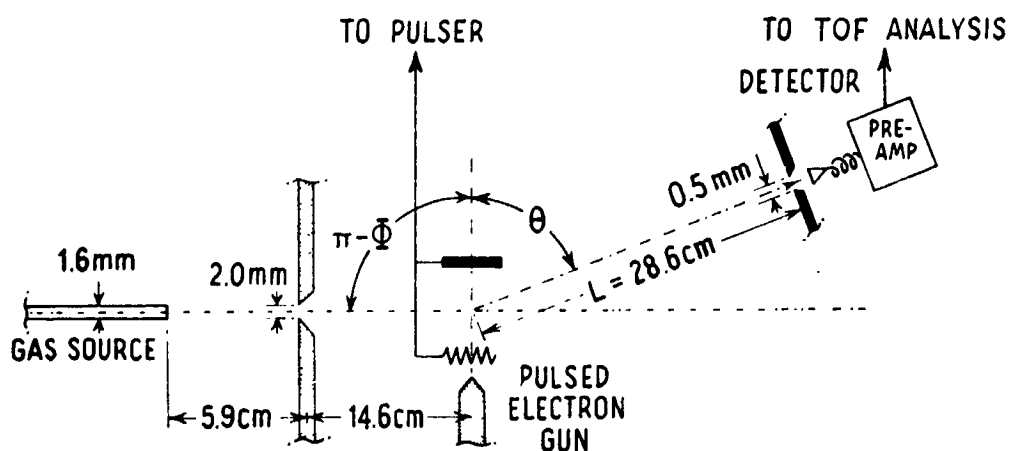
Figure 2.1 Experimental arrangement for time-of-flight measurements.

beam, nominally perpendicular to the electron beam ($\Phi \approx 90°$; see Figure 2.1), has an angular divergence of about three degrees. Samples of data taken at two different angles θ are plotted as points in Figure 2.2. Striking features of the results when compared with what would be found if recoil effects were negligible (curve c in Figure 2.2) include:

   1. The narrowness of the distributions.

   2. The presence of two peaks.

   3. The sensitivity of the position of the distribution to the angle of deflection.

Simple kinematic considerations (Warnock and Bernstein, 1968) can be used to explain these velocity distributions.
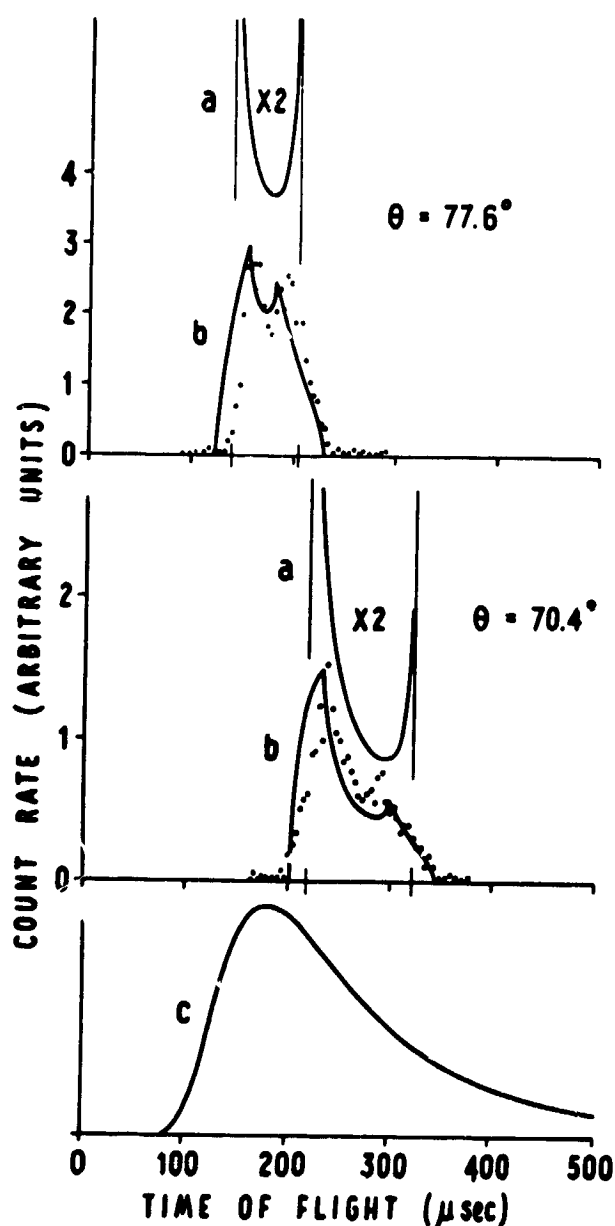
Figure 2.2 Time-of-flight spectra for metastable 2^3S_1 helium.
Points represent experimental data. Curves a are theoretical
for perfect collimation (vertical lines indicate cutoffs);
curves b are theoretical, accounting for 3° angular divergence
in the incoming, ground state beam. Curves a and b are cal-
culated assuming that the electron energy is 0.75 eV above
threshold. Curve c is theoretical if recoil effects are
neglected.

2.2 THEORETICAL

For an idealized experiment in which the electron gun is operated in either an instantaneous pulse or DC mode, the distribution function $g(\bar{v})$ of metastable atoms is related to the distribution function $f(\bar{v}_o)$ of the ground state atoms by

$$g(\bar{v}) = \frac{j}{e} \, \sigma \int d^3v_o \; f(\bar{v}_o) \; p(\bar{v}_o,\bar{w}) \tag{1}$$

where j is the electron current density at the point of interaction, e is the electronic charge, σ is the total metastable excitation cross section (assumed independent of $\bar{v}_o$), and $p(\bar{v}_o,\bar{w})$ is the probability density that a metastable produced from a ground state atom having initial velocity $\bar{v}_o$ will have velocity $\bar{w}$ in the center of mass frame of the electron and the atom; the normalized differential excitation cross section is included in $p(\bar{v}_o,\bar{w})$. The variables $\bar{v}$, $\bar{v}_o$ and $\bar{w}$ are related through conservation laws.

For s-wave scattering, the law of conservation of energy shows that $p(\bar{v}_o,\bar{w})$ may be well approximated by

$$p(\bar{v}_o,\bar{w}) = \frac{1}{4\pi V^2} \, \delta(w-V) \tag{2}$$

where V is the recoil speed of the metastable in the center of mass system:

$$V = \mu \sqrt{\frac{2\Delta E}{m}} \tag{3}$$

11
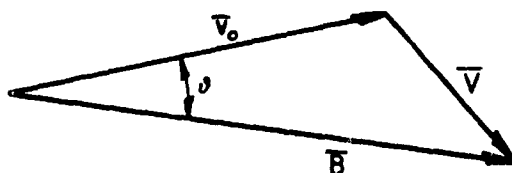
Figure 2.3 Diagram showing relation of vector variables.

Here ΔE is the electron's excess energy above the excitation threshold*, μ is the electron-atom mass ratio, and m is the mass of the electron.

From the law of conservation of momentum, we may define a vector $\bar{B}$ (Figure 2.3) which is constant for a given laboratory velocity $\bar{v}$ of the metastable

$$\bar{B} \overset{\Delta}{=} \bar{v} - \mu\bar{u}_o = \bar{v}_o + \bar{V} \tag{4}$$

Here $\bar{u}_o$ is the incident velocity of the electron. From this one may write

$$V^2 = B^2 + v_o^2 - 2\bar{B} \cdot \bar{v}_o \tag{5}$$

Converting the delta function from w (center of mass system) to v_o (laboratory system) variables, we have

$$\delta(w-V) = \frac{\delta(v_o - v_o^+) + \delta(v_o - v_o^-)}{|\hat{v}_o \cdot \hat{V}|} \tag{6}$$

---

* Terms on the order of the electron-atom mass ratio and of the order of the atom-electron speed rat.) are neglected with respect to unity throughout.

12

where the carats indicate unit vectors, and

$$v_o^{\pm} = B \cos \vartheta \pm \sqrt{V^2 - B^2 \sin^2 \vartheta} \qquad (7)$$

Suppose now that the ground state beam is produced from a Maxwellian gas. Then

$$f(\vec{v}_o) = \frac{n_o}{\pi^{3/2} \alpha^3} \exp[-v_o^2/\alpha^2] \qquad (8)$$

so that Equation 1 may be rewritten in the form

$$g(\vec{v}) = \frac{j}{e}\sigma \cdot \frac{n_o}{\pi^{3/2} \alpha^3} \cdot \frac{1}{4\pi V^2} \int_{\Omega_o} d\omega_o \frac{v_o^{+2} \exp[-v_o^{+2}/\alpha^2] + v_o^{-2} \exp[-v_o^{-2}/\alpha^2]}{|\hat{v}_o \cdot \hat{v}|} \qquad (9)$$

where Ω_o is the solid angle defined by the intersection of the ground state beam and the sphere of integration in v_o space, which is determined by the conservation laws (see Equation 6 and Figure 2.4).

2.2.1 Collimated Beams

If the ground state beam is perfectly collimated, the integral in Equation 9 degenerates, and the distribution function of metastable atoms is given by the integrand. Curves $\underline{a}$ of Figure 2.2 show predicted time-of-flight curves for a perfectly collimated ground state beam, using the parameters indicated in Figure 2.1 (the time-of-flight distribution, h(t), is related to the distribution function by

$$h(t) \propto \frac{x^3}{t^4} g(\frac{x}{t}) \qquad (10)$$

13
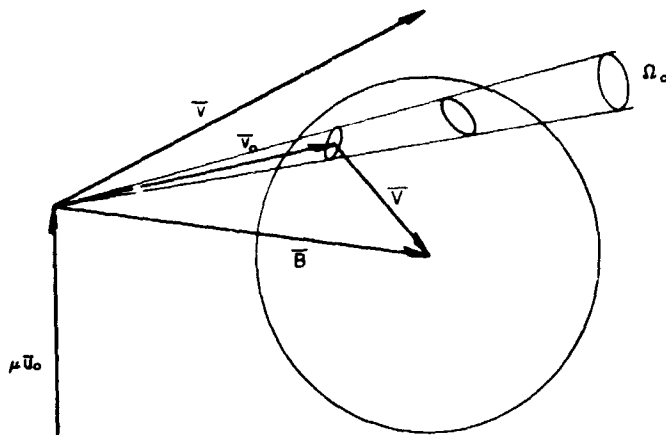
Figure 2.4 Velocity space diagram showing contributing portion of the sphere of possible values of $\bar{v}_o$ for a ground state beam of solid angle Ω_o.

where x is the distance from the excitation region to the point of observation).

The sharp cutoffs and the accompanying singularities arise from the vanishing of the denominator in the distribution. Their physical origin can be seen from Figure 2.4 and from the definition of the vector $\bar{B}$ (Equation 4). The tip of $\bar{B}$, which defines the center of the "contributing" sphere, moves parallel to $\hat{v}$ as the magnitude of $\bar{v}$ increases. Metastables are only observed in the velocity range for which the ideal ground state beam intersects the contributing sphere; hence the existence of cutoffs. The maxima in the distribution occur when the beam is tangent to the sphere, i.e., when $\bar{v}_o \cdot \bar{V} = 0$, since surface elements on this part of the sphere contribute most efficiently to the resultant distribution.

The cutoff velocities can be calculated in a straightforward manner. For the special case of the present experiment (detector coplanar with the incident beams) the limiting velocities are given by

14

$$v_{\substack{max \\ min}} = [\mu u_o \sin\Phi \pm V]\csc(\Phi-\Theta) \quad \begin{cases} \Theta < \Phi \\ V < \mu u_o \sin\Phi \end{cases} \quad (11)$$

The cosecant term explains the strong shift of the distribution with relatively small angular changes (see Figure 2.2).

The cosecant dependence of the cutoffs on Φ (or Θ) also indicates that the simple integrand approximation to the distribution is inaccurate if the beam divergence (or detector width) is any greater than about a degree. Numerical integrations for the conditions of the present experiment (beam divergence $\Delta\Phi\approx3°$; detector width negligible, $\Delta\Theta\approx0°8'$) are shown as curves $\underline{b}$ in Figure 2.2.

The principal effects of finite beam divergence are seen to be:

    i)   a widening of the distribution;

    ii) a narrowing of the peak separation;

    iii) a tendency for the peaks and valley of the distribution to "average out."

As the beam divergence increases, these effects eventually lead to a distribution with a single peak. Indeed, applying a 6° divergence to a hot hydrogen beam closely reproduces the measured velocity distribution approximated analytically by $v^4 \exp[-v^2/\alpha^2]$ in the work of Shyn et al., (1969).

2.2.2 Diffuse Sources

In the limit of a completely uncollimated ground state beam, where the gas enters the electron beam uniformly from all directions, Equation 9 can be integrated analytically.

The resulting distribution function is

$$g(\bar{v}) = \frac{j}{e} \, \sigma \, \frac{n_o}{\pi^{3/2} \alpha^3} \, \exp[- \frac{B^2 + V^2}{\alpha^2}] \, \frac{\sinh \frac{2BV}{\alpha^2}}{\frac{2BV}{\alpha^2}} \qquad (12)$$

This expression reduces to a Maxwellian distribution only when the following conditions hold simultaneously:

   i)   the energy E of the incident electron is equal to the excitation energy of the metastable state;

   ii) $\theta = 90°$.

The behavior of a metastable helium (2^3S_1) velocity distribution for electrons having threshold energy is illustrated in Figure 2.5, the curves having been normalized to identical peak values. As the angle of observation θ shifts from zero to 180°, it is seen that the distribution shifts from "wide and fast," through Maxwellian, to "narrow and slow." Figures 2.6 and 2.7 show, respectively, the behavior of the peak intensity and position of the distribution given by Equation 12.

    Although the approximation of s-wave scattering is known to be poor for helium (Ehrhardt and Willmann, 1967; Ehrhardt et al., 1968) the above calculation is useful since it provides a meaningful limiting case. Another interesting extreme case is that of perfect forward scattering of the electrons. In this case the distribution becomes

$$g(\bar{v}) = \frac{j}{e} \, \sigma \, \frac{n_o}{\pi^{3/2} \alpha^3} \, \exp[-D^2/\alpha^2] \qquad (E \rightarrow \infty) \qquad (13)$$

where

$$\bar{D} = \bar{v} - (\mu u_o - V)\hat{u}_o \qquad (14)$$

16

NORMALIZED
VELOCITY
DISTRIBUTION
(ARBITRARY
UNITS)

$\propto (\frac{V}{\alpha})^2 g(\frac{V}{\alpha})$

$\theta:$ 180° 90° 0°

DETECTOR

NORMALIZED VELOCITY v/α
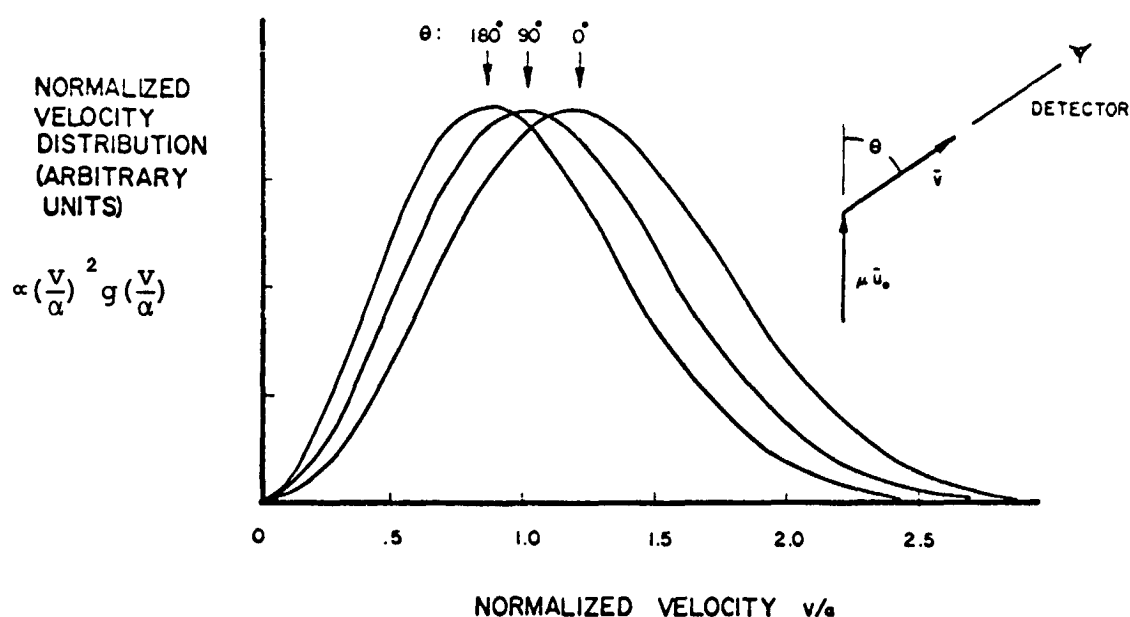
Figure 2.5 Velocity distributions for 2^3S helium at various detector
positions. Arrows indicate peak positions. Incident electrons
assumed to have threshold energy. Source gas assumed to have (diffuse)
Maxwellian velocity distribution.

In this limit (large electron energy) V approaches μu_o, so
that the distribution approaches Maxwellian everywhere. It
is therefore concluded that the distribution function in beams
of metastable atoms produced by electron impact from Maxwellian
ground state sources should vary between the two-peaked pre-
dictions of the integrand of Equation 9 and the isotropic
Maxwellian case of Equation 13.

2.3 EFFECTS OF DIFFERENT EXCITATION ENERGIES and/or MOLECULAR
     MASSES

Figures 2.2, 2.5, 2.6 and 2.7 demonstrate properties of the

17
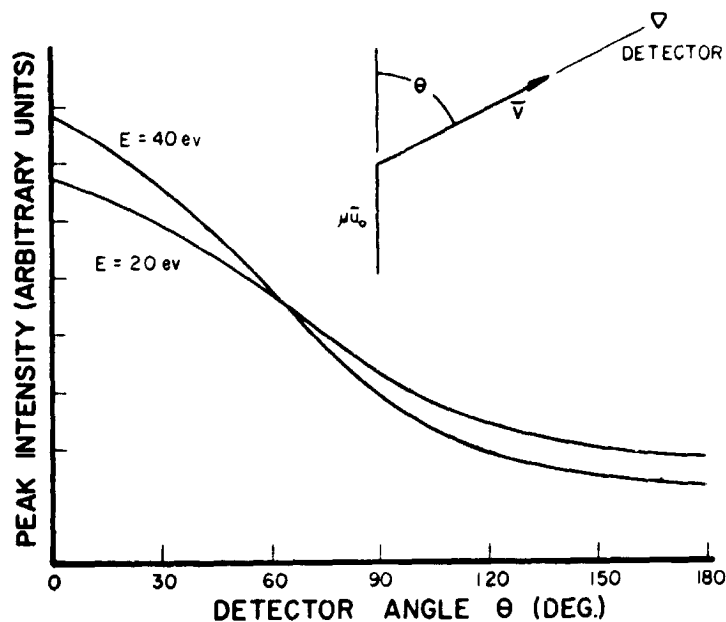
Figure 2.6 Peak intensity for 2^3S helium velocity distribution vs. angular position θ of detector; energy E of incident electrons is parameter. Source gas assumed to have (diffuse) Maxwellian velocity distribution.
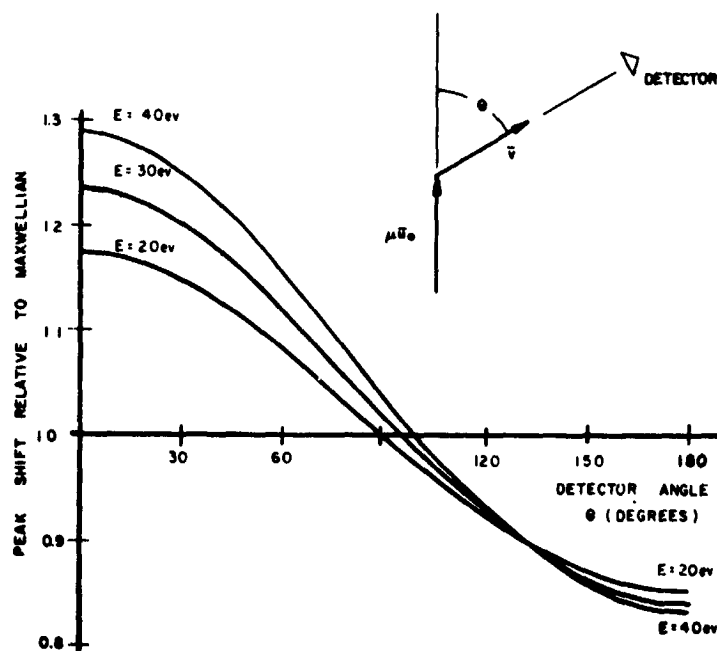
Figure 2.7 Peak shift for 2^3S helium velocity distribution vs. angular position θ of detector; energy E of incident electrons is parameter. Source gas assumed to have (diffuse) Maxwellian velocity distribution. Shift evaluated relative to velocity peak of source gas ($v_{peak,source} = \alpha$; $\alpha = \sqrt{2kT/M}$).

velocity distribution for 2^3S_1 helium. The effects of using different gases or of exciting different states have not been indicated. An informative means for comparing such effects is the following.

Curve $\underline{c}$ of Figure 2.2 would represent the expected time-of-flight spectrum for $2^3S_1'$ helium if recoil effects were totally absent; the spectrum is characteristic only of the thermal distribution of velocities in the ground state gas. Therefore, if the time axis is properly scaled using the most probable velocity of particles in the gas, the resulting curve may be considered universal, i.e., valid for all gases. Curves $\underline{a}$ of Figure 2.2, however, do not acquire a similar universal character, since they are strongly dependent on recoil effects. As a consequence of this, useful information on the degree to which beams of metastables produced from various gases are distorted by recoil can be obtained by determining the conditions which produce the illustrated "shifts" of curves $\underline{a}$ relative to the universal curve $\underline{c}$.

Curves $\underline{a}$ are characterized by their cutoffs. Let the cutoff velocities be normalized with respect to the most pro-bable velocity in the ground state gas. For the given shifts in helium, it is now possible to determine the angles and energy excesses which will produce identical relative shifts with respect to curve $\underline{c}$ for gases of arbitrary mass and ex-citation energy. Set $\Phi = \frac{\pi}{2}$ in order to correspond with the helium experiment. In addition, consider the source gases to have a fixed temperature (T = 300°K for the helium results). Then, for a given relative position of an $\underline{a}$-type spectrum,

19

i.e., for fixed v_{max}/α and v_{min}/α, the cutoff relations (Equation 11) can be inverted to give

$$\frac{\Delta E}{E^*} = \text{const.} = \frac{(\Delta v)^2}{(\Sigma v)^2 - (\Delta v)^2} \qquad (15)$$

and

$$\sqrt{\frac{M}{E}} \cdot \sin\left(\frac{\pi}{2} - \theta\right) = \text{const.} = \frac{2}{\Sigma v}\sqrt{\frac{m}{kT}} \qquad (16)$$

where

$$\Sigma v \triangleq \frac{v_{max} + v_{min}}{\alpha}$$

$$\Delta v \triangleq \frac{v_{max} - v_{min}}{\alpha} \qquad (17)$$

and E is the energy of the incident electron. Equation 15 says that, for states of a fixed excitation energy E^*, a fixed energy excess ΔE will produce a spectrum with the same "shift" relative to curve c regardless of the mass of the atom or molecule. Note, however, that Equation 16 states that the angle at which such a spectrum is observed does depend on the mass of the excited particle.

Calculated deflection angles and energy excesses for various gases are shown in Table 2.I. As expected, these results show that the deflection of the metastable beam is much less for N_2 than for helium. This distortion will decrease further as the mean velocity of the ground state beam is increased.

Finally, it should be noted that if the energy of the incident

20

electrons is sufficient to excite states which may <u>decay</u> to a metastable level, the resulting velocity distribution will be a weighted sum of distributions due to all such levels; kinematically, these levels must be treated in exactly the same manner as the metastable levels themselves (using the relevant excitation energy), since the recoil from the cascade photon is negligible.

State	Atomic Mass Number	Excitation Energy E^*(eV)	Deflection Angle $(\frac{\pi}{2} - \theta)_{fast}$	$(\frac{\pi}{2} - \theta)_{slow}$	Energy Excess ΔE(eV)
$He(2^3S_1)$	4	19.82	12.4°	19.6°	0.75
$H_2(c^3\pi_u)$	2	11.86	13.6°	21.5°	0.45
$D_2(c^3\pi_u)$	4	11.86	9.6°	15.0°	0.45
$N_2(A^3\Sigma_u^+)$	28	6.16	2.6°	4.1°	0.23
$N_2(a^1\pi_g)$	28	8.54	3.1°	4.8°	0.32
$N_2(E^3\Sigma_g^+)$	28	11.87	3.6°	5.6°	0.45

Table 2.I   Observation (deflection) angles and energy excesses which lead to the same relative structure in the time-of-flight spectra as indicated for helium by curves <u>a</u> and <u>c</u> in Figure 2.2.

2.4 CONCLUSIONS

The results of this section show that the effects of recoil on the velocity distribution of the metastable molecules are understood. Inverting the measured distributions to obtain the ground state velocity distribution requires an

analysis very similar to the above. Since the form of the

distributions expected from the satellite experiment is

unknown, this inversion will have to be carried out numerically.

3. EFFECTS OF SHORT-LIVED METASTABLE STATES ON THE INTERPRETATION OF VELOCITY DISTRIBUTIONS IN N_2 BEAMS.

If the excited state of a molecule used in MTOF studies has a very long lifetime relative to the time it takes to drift from the electron gun to the detector, then the meta-stable beam can be described in terms of geometric and kine-matic effects (Section 2). If, however, the lifetime of the state is so short that a significant fraction of the metastables decay in transit to the detector, then the observed distribution will be deficient in the more slowly moving excited molecules. Thus, a knowledge of the lifetime of the metastable state is necessary in order to correctly deduce the velocity distribution in the parent beam.

3.1 APPARATUS AND METHOD

The apparatus shown in Figure 3.1 is set up to mea-sure the lifetime of the $a^1\pi_g$ metastable state of molecular nitrogen. The setup is similar to those used in the other time-of-flight experiments discussed in this report, except that the detector is mounted on a carriage, enabling it to be translated along the axis of the beam. The velocity selector shown in the figure is to be used in refinements of the present experiments; it was withdrawn from the beam path and was not used to obtain any of the data presented here.

23
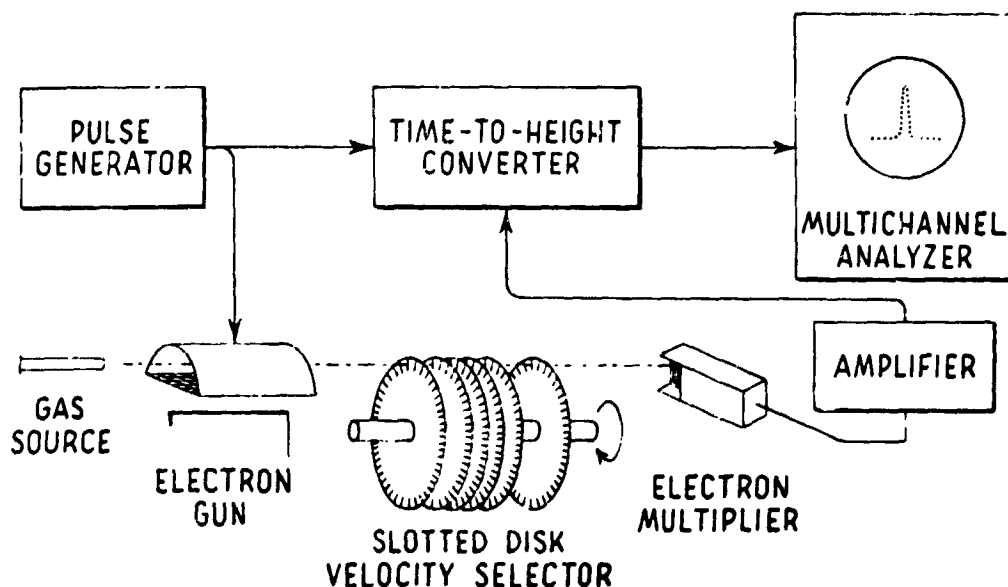
Fig. 3.1 Experimental arrangement for lifetime measurements.

Two types of experiments were conducted, both of which can be used in principle to determine metastable lifetimes. The first uses the time-of-flight technique; the second uses the drop in total metastable signal with electron gun-detector distance.

3.1.1 The Time-of-Flight Method

In using the time-of-flight technique, molecular nitrogen is excited by pulsed electron bombardment (pulses typically 30v amplitude, 30μsec duration), and the time-of-flight distribution is measured at a fixed detector position (about 30 cm from the electron gun). The deviation from the distribution obtained when no decay occurs is then a measure of the lifetimes of the various short-lived metastable states.

24

The time-of-flight distribution expected in the absence of metastable decay can, in principle, be calculated by the methods outlined in Section 2. However, since the exact spatial distribution of the ground state gas in the electron gun is unknown in this experiment, the TOF distribution for a nondecaying beam is obtained experimentally using argon as the source gas.

The metastable states in argon are very long lived (Muschlitz, 1968), so that negligible decay of metastables occurs between the electron gun and the collector. A measured time-of-flight spectrum for metastable argon is shown in Figure 3.2. It was found empirically that this distribution can be closely fitted by an expression of the form

$$h_{Ar}(t) \propto \frac{x^{n+1}}{t^{n+2}} \exp \left[- \frac{x^2}{\alpha_{Ar}^2 t^2} \right]$$

where α_{Ar} is the most probable speed in the ground state argon gas; the exponent n, determined by fitting the data, is found to be equal to three within experimental error. The solid curve in the figure represents this distribution.

This same functional form for the TOF distribution, modified by the inclusion of decay terms (Freund and Klemperer, 1967; Zorn and Pearl, 1967), is next applied to the nitrogen data:

$$h_{N_2}(t) \propto \frac{x^{n+1}}{t^{n+2}} \exp \left[- \frac{x^2}{\alpha_{N_2}^2 t^2} \right] \left\{ N_a \exp\left[- \frac{t}{\tau_a} \right] + N_A \exp \left[- \frac{t}{\tau_A} \right] \right\}$$
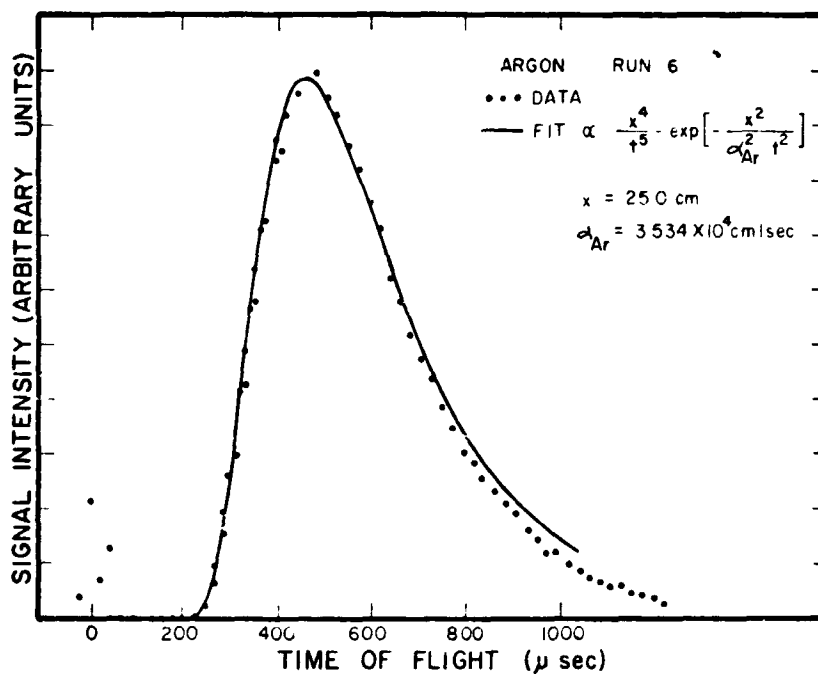
Figure 3.2 Measured time-of-flight spectrum for metastable argon and fitted curve.
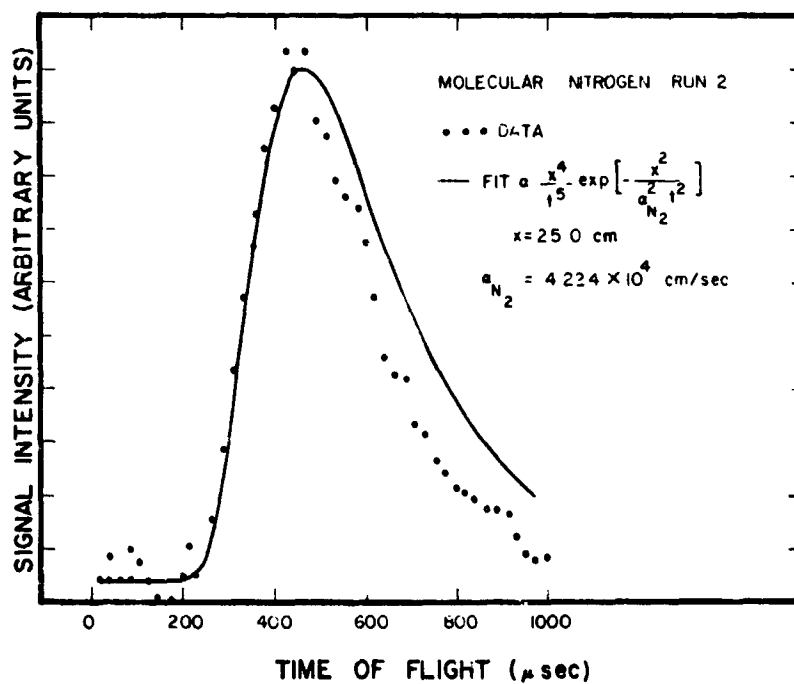
Figure 3.3 Measured time-of-flight spectrum for metastable nitrogen and curve expected in the absence of decay in flight.

26

Here N_a and N_A are the populations of $a^1\pi_g$ and $A^3\Sigma_u^+$ metastables in the beam when it leaves the electron gun; τ_a and τ_A are the mean lifetimes of the two states. Experimental data and the curve expected in the absence of decay are shown in Figure 3.3. A marked discrepancy between the data and the curve is observed, as expected.

Since the lifetime τ_A is of the order of one second (Muschlitz, 1968), the loss of $A^3\Sigma_u^+$ metastables from the beam is negligible over the flight times typical of this experiment ($\approx 10^{-3}$ sec). Consequently, the second exponential may be replaced by unity. The remaining lifetime τ_a and the population ratio N_a/N_A are then picked to give the best fit to the experimental data; the fitted lifetime is in agreement with the value $\tau_a = 1.7 \times 10^{-4}$ sec obtained by Lichten (1957). Further refinements in the experiment are expected to yield an improved value of this lifetime.

3.1.2 The Decay-with-Distance Method

In the experiment utilizing the decay of total metastable signal with distance, the electron gun is used in the DC mode. Once again argon is used as the calibrating gas; in this case, it is expected that no decay in total beam intensity should be observed as the detector is moved. For molecular nitrogen, however, the signal should fall off with distance in a manner related to the lifetimes of the metastable states in the beam (Lichten, 1957).

27
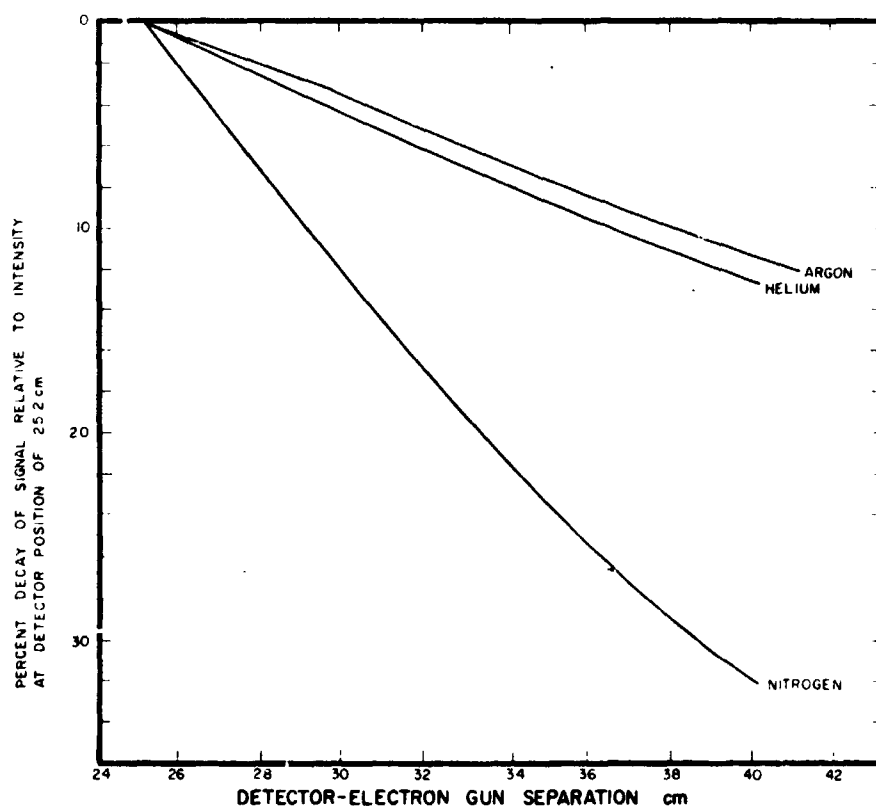
Figure 3.4   Measurements of beam strength as a function of detector position; results are shown for argon, helium and molecular nitrogen.

Experimental data are shown in Figure 3.4.   The pronounced fall-off of the argon curve (and of the curve for helium, which was taken to qualitatively verify the phenomenon) is, of course, unrelated to a finite metastable lifetime.   This change in intensity must, however, be understood in order to accurately measure lifetimes; we believe that the causes of the intensity change are geometric spreading of the beam, quenching due to collisions in the beam, and a change of detector efficiency with position due to spatially varying stray magnetic fields.

28

The data for nitrogen shown in the same figure show a much more dr..tic fall-off with distance, the difference between the argon and nitrogen curves being due to decay of the metastables along the beam. This decay can be essentially ascribed to the decay of the $a^1\pi_g$ state, yielding a lifetime in rough agreement with that measured by Lichten (1957).

3.2 COMMENTS AND CONCLUSIONS

In interpreting the data from the above experiments, it has been assumed that cascading from higher excited levels into the $a^1\pi_g$ metastable state lasts no longer than a few microseconds after excitation; further, it is assumed that $a^1\pi_g$ and $A^3\Sigma_u^+$ are the only two metastable states populated in the beam. These assumptions may have to be reexamined in light of recent work by Freund (1969a, 1969b). However, the time-of-flight data obtained in the laboratory are sufficient to make empirical corrections to measured TOF spectra, allowing the velocity distribution in the ground state beam to be determined.

4. DIRECTIONAL SENSITIVITY OF MTOF ANALYZERS

4.1 INTRODUCTION

By using a small electron beam and a small detector, the MTOF method can provide good directional resolution of the incoming ground state beam, since the reccil effects on rapidly moving N_2 molecules are small (see Section 2). In the satellite experiment however, it is desirable to use an electron beam of large cross section and a detector of large area in order to improve the data counting rate; large areas, unfortunately, lead to a loss of angular resolution. The conflict between the requirements of good angular resolution and of large excitation and detector areas can be resolved in a simple manner by collimating the gas beam <u>after</u> it is excited.

This can be done by introducing an array of metallic tubes with the desired acceptance angle between the electron gun and the detector. Since metastables striking the walls of such tubes are very efficiently quenched (Donnelly, et al., 1969a), only the excited molecules which pass through the array without touching the walls, i.e., within the desired angular divergence, can be counted by the detector (the quenched molecules which emerge from the tubes more or less diffusely are in their ground states and cannot trigger the detector; thus, they are not counted); see Pichlik and Zorn, 1970.

30

4.2 EXPERIMENT

The experiment utilizes the standard MTOF arrangement, except that the gas enters the system through small holes, and that the metastable beam is collimated by an array of fine metal tubes; in addition, the entire detector system can be rotated about its midpoint (Figure 4.1). The sources used for these experiments are located in a plane, with angular separations of 6°.

The direction of maximum sensitivity and the angular resolving power of the analyzer system is related to the bore-to-length ratio d/L of the collimating tubes. If this ratio is small, the analyzer will allow molecules from one source to be detected and counted, while those from another source only a few degrees away will not be detected. Rotating the analyzer and observing the change in the counting rate allows the angular separation of the sources to be determined.

The test gas used in these experiments is argon. During operation, the electron gun provides 50μsec pulses of 30 volt electrons at a repetition rate of 500 Hz. The pulses during each gun pulse (due to photons) are blocked, and the angle θ (see Figure 4.1) is varied slowly and uniformly while the multichannel analyzer, operating in the multiscaling mode, steps from one channel to the next for storage of the data. Since each channel corresponds to a different direction, the peaks in the counts/channel distribution show the angular position of the gas sources,

31
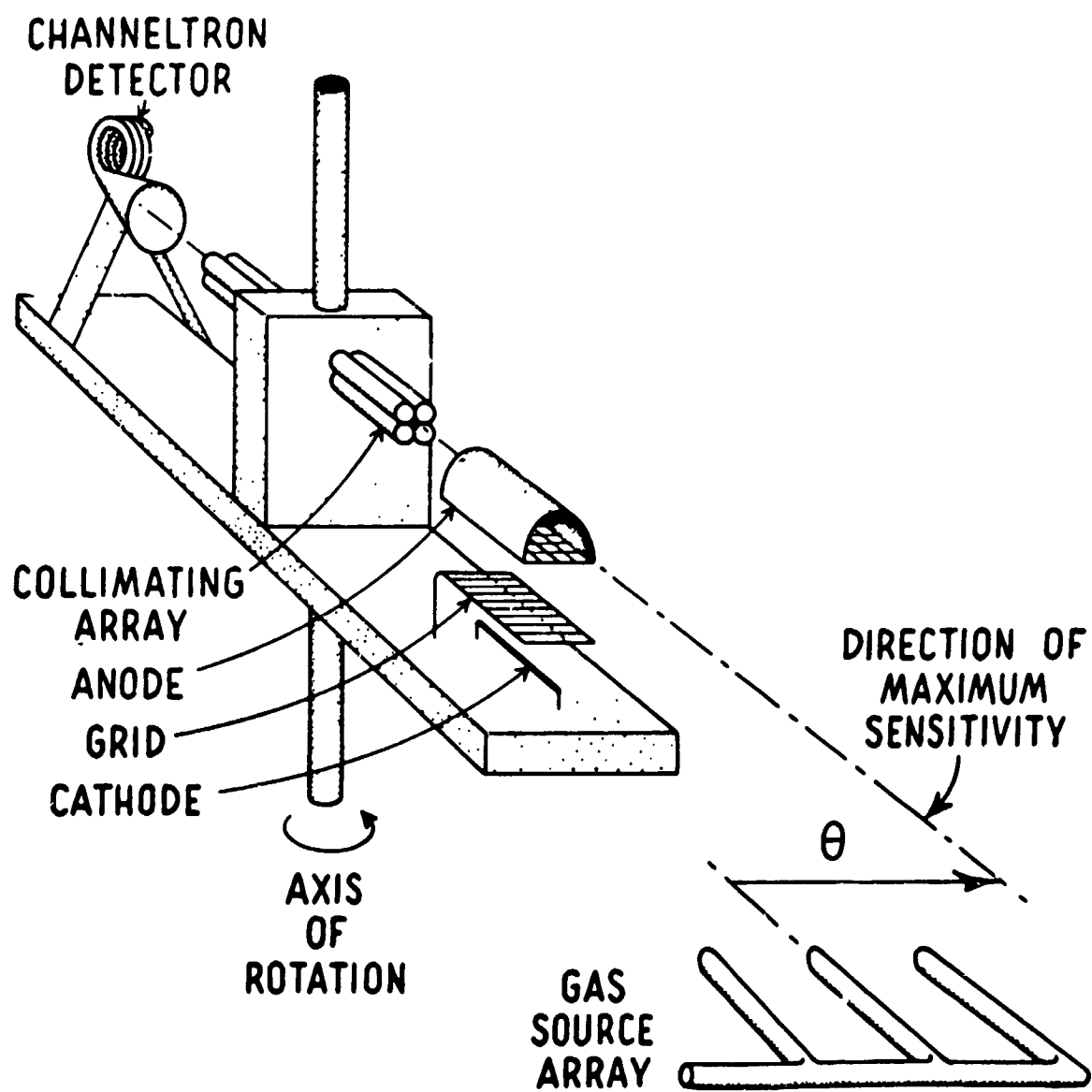
Fig. 4.1 Functional block diagram of directional gas analyzer.

32

with halfwidths characteristic of the resolving power of the collimating array.

4.3 CONCLUSIONS

The results shown in Figure 4.2 indicate that the directional sensitivity of a simple metastable time-of-flight system is significantly better than 6°. A more refined determination of the effects of the collimation system on the angular resolution of metastable time-of-flight systems is currently in progress.
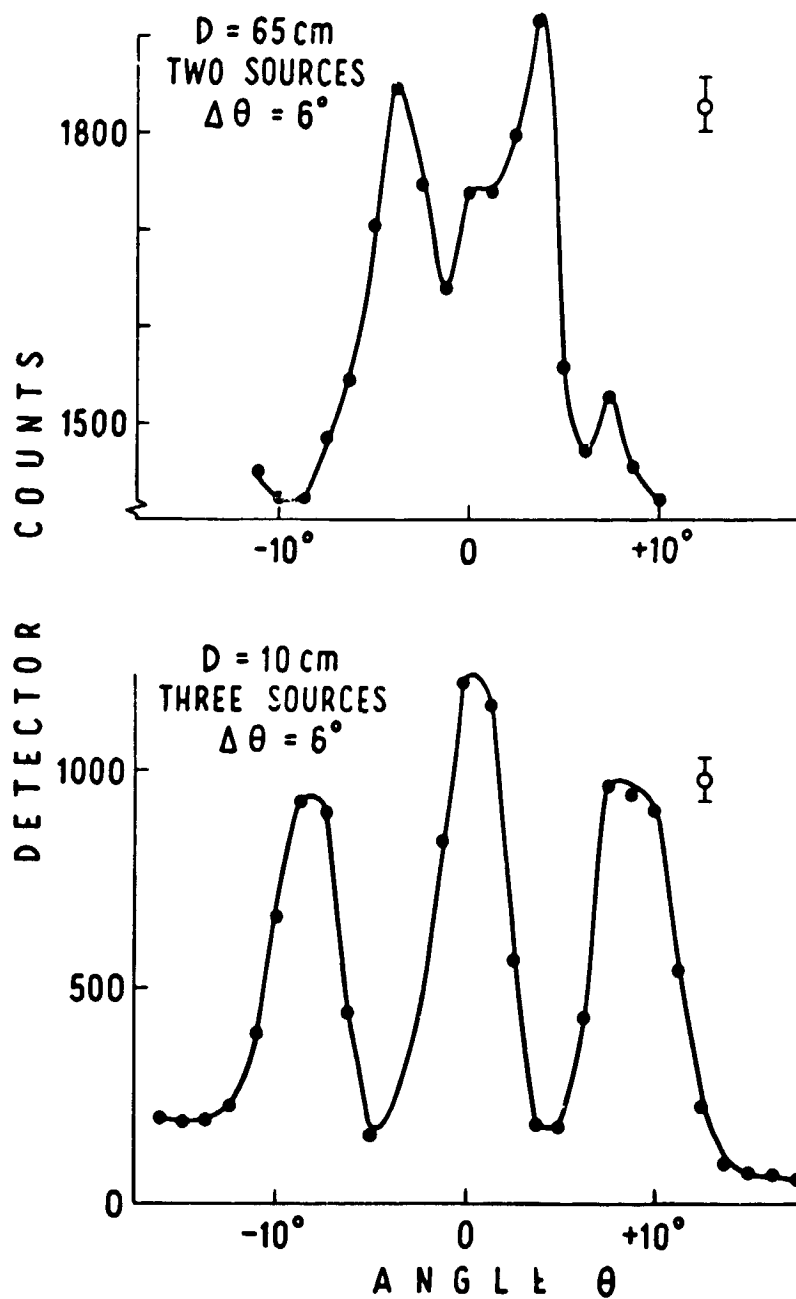
Figure 4.2 Counts vs. directional gas analyzer (DGA) direction θ. θ is measured from an arbitrary reference line. D is the distance from the source to the DGA; Δθ is the known angular separation of the sources. The upper figure is for two sources; the lower figure is for three sources.

34

5. CHANNEL MULTIPLIERS FOR DETECTION OF METASTABLE MOLECULES

5.1 INTRODUCTION

A metastable atom or molecule usually de-excites upon
striking a conducting surface. If the energy of the molecule's
metastable state exceeds the work function of the surface,
there is a probability on the order of a few percent that the
de-excitation will be accompanied by the ejection of an
electron from the surface (Hagstrum, 1960; Kaminsky, 1965;
Prince, 1968). This Auger process can be used as the basis
of a detector for weak beams of neutral, metastable mole-
cules if the ejected Auger electrons are efficiently counted.

Direct multiplication of the Auger electrons can be
employed to construct a sensitive and fast-responding detector;
the metastable molecules are allowed to strike the cathode
of a windowless electron multiplier so that almost every
Auger electron ejected from the cathode will yield an out-
put pulse from the multiplier. The pulses can be integrated
and measured as a current if desired; however a main ad-
vantage of the direct multiplication method is that digital
circuits can be used to process the output pulses if their
rate is below 10^6/sec. The use (Goodrich and Wiley, 1962;
Evans, 1965) of a continuous channel electron multiplier
(Bendix Channeltron) for the detection of weak beams of
metastable molecules is discussed in this section. Compared
to the multiple dynode (Bingham, 1966) and strip dynode
(Goodrich and Wiley, 1961) multipliers which have been used

35

in this application, the continuous channel multiplier has
the advantages of lower noise, simpler circuitry, and smaller
size. In fact, since very compact and dense arrays of
channel multipliers have proven practical for image inten-
sification (Goodrich et.al., 1967), it should be feasible to
do molecular scattering experiments in which an array of
fifty or more channel multipliers acquires data simultaneously
over a wide range of angles.

5.2   EXPERIMENT

Generally, experiments are done in vacuum systems
which are evacuated to a base pressure on the order of 10^{-7}
torr by oil diffusion pumps; during the measurements, the
partial pressure of the gas under study sometimes exceeds
1×10^{-5} torr in the entire vacuum chamber. Liquid
nitrogen traps are often used during runs, but no unusual
care is taken to keep forepump or diffusion pump vapors
from backstreaming into the systems during pumpdown. The
detector output pulses are coupled to external circuitry
using an emitter follower (Figure 5.1) which is mounted with
the channeltron inside the vacuum chamber.

5.3   RESULTS

In the course of experiments performed in this
laboratory (Crosby and Zorn, 1969; Donnelly et al., 1969),
thermal beams of metastable helium (20 eV), neon (16.5 eV),
argon (11.5 eV), krypton (9.9 eV), xenon (8.3 eV), and molecular
nitrogen (8.5 and 6.2 eV) have been detected (the numbers in
parentheses are approximate energies of the metastable
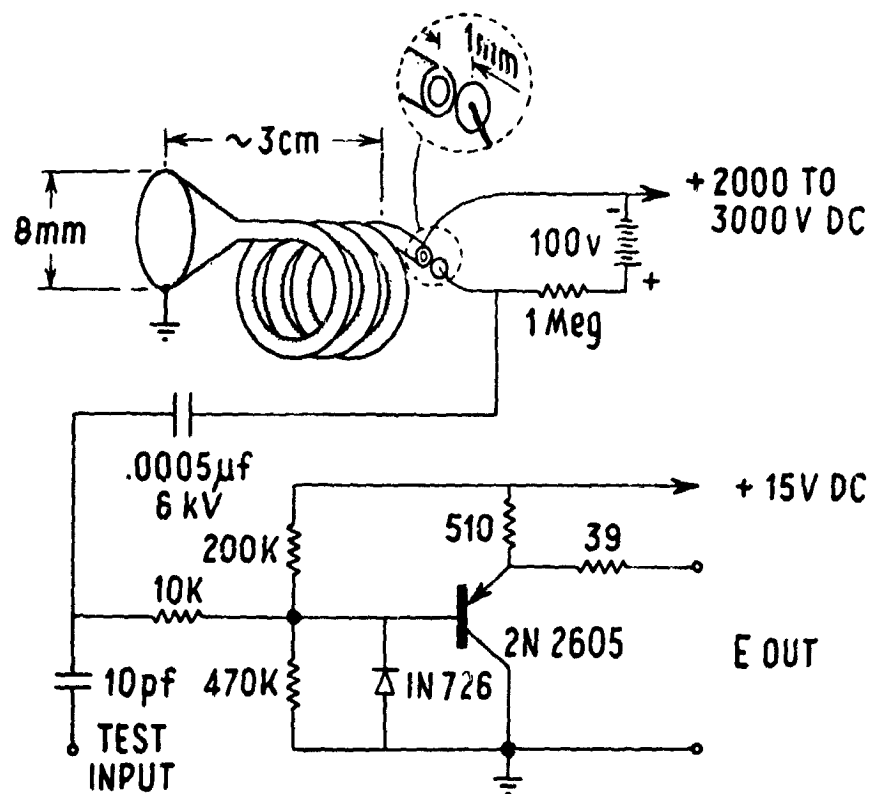
Figure 5.1 The Channeltron output is picked up by a small metal button and fed to the input of an emitter follower which is mounted together with the multiplier inside the vacuum chamber. The circuit serves as an impedance transformer so that the signal pulses can be brought out through long, low impedance leads. With 2.1 kV on the multiplier, the emitter follower output pulses have an amplitude of 0.05 V and a rise time of less than 100 nanoseconds. We are indebted to James Svenson for suggesting this design.

states). Although the yield of Auger electrons per meta-
stable molecule incident on the Channeltron cathode has not
been measured here, it is judged that the yield is comparable
to that achieved on the tungsten or platinum surfaces used in
the conventional Auger detectors (Kaminsky, 1965), that is
about 25% of any helium metastables incident on the Channeltron
cathode will yield an output pulse from the multiplier. As one
would expect, molecules with less energetic metastable
states are detected less efficiently; metastable xenon, for
example, seems to be detected about one percent as efficiently
as is metastable helium (see also Prince, 1968). Molecules
with metastable states less than 6 eV above the ground state
will probably not be detected by the Channeltron. The
detection efficiency of a Channeltron for a given metastable
species seems to remain within ten per cent or so of an
equilibrium value in spite of exposure of the multiplier
to humid air and backstreaming pump vapors.

The usual background signal, or dark current, in the
Channeltron multiplier is 0.1 counts/sec or less, so it is
feasible to do experiments with beam signals as low as 1 count/
sec. To maintain a low background count rate it is essential
to keep ultraviolet radiation (as from bare filaments), and
ions (as from vacuum gauge tubes) out of the multiplier.
Windows in the vacuum system need not be covered during the
experiments, however, since the multiplier does not respond
to visible light.

38

As stated above, the normal cathode of the Bendix
multiplier will not yield Auger electrons for metastable
molecules with excited states of energy less than about
6 eV. However, it has been found (Lichten, 1958; Lurio,
1962) that a coating of an alkali metal suffices to lower the
cathode's effective work function to the neighborhood of
3 eV. The surprising aspect of this process is how little
alkali is required to make the Channeltron sensitive to, say,
room light transmitted through a plexiglas window. During
experiments in this laboratory, a sodium molecular beam
oven has been used in a vacuum system with several optical
baffles between the sodium source and the multiplier. With
all of this shielding, however, a substantial sensitivity
of the multiplier to room light occurs within a few minutes
of turning on the sodium beam. Thus, it is extremely easy
to extend the range of multiplier response without running
the risk of exposing the multiplier directly to an intense
beam of the alkali metal. It is found, however, that the sen-
sitivity of such a surface decays an hour or so after the
oven is turned off, or after the system is opened to air.
Consequently, continued deposition of the alkali at a low
rate is required if the Channeltron is to be used over
extended periods in a sensitized state.

Occasionally a Channeltron develops erratic gain or a
very high noise level. This can come from mistreatment,
such as overloading due to high counting rates, or from

causes which are less obvious. It is usually possible to restore such a multiplier to good operating condition by flushing it thoroughly with acetone or ethyl alcohol and letting it rest on the shelf for a few days. In fact, one Channeltron has been resuscitated in this manner after it had failed from a corona discharge that occured when the system vacuum was lost with 2.1 kV still applied to the multiplier. A noisy or inoperative multiplier should not be discarded before a few of these remedies have been tried.

The countinuous channel multipliers are made of glass tubing which can be broken if too much stress is exerted by the mount; once the multiplier is in place, however, the assembly is not overly delicate. Mounts in this laboratory are made from pieces of Teflon; at other laboratories these multipliers have been potted in epoxy resin. It is useful to know that pieces of a broken Channeltron can sometimes still be used for electron multiplication, albeit with lower gain, if new electrical connections for the DC voltage are made to the resistive glass tube with conducting paint.

5.4 DISCUSSION

We have made extensive use of the Bendix Channeltrons in our work with metastable molecules. They have proven to be very satisfactory for operation in the laboratory.

Indications are favorable (Smith, 1966; McCullough, 1968; Frank et al., 1969) that their long-term (1 month continuous use) reliability may be satisfactory for use in satellite

experiments.   However, a careful study of the available

windowless electron multipliers needs to be made before

proceeding with the construction of an experiment which is

to function continuously for weeks at a time (Cone, 1967).

In addition to the Bendix Channeltron, the multipliers to be

considered include the continuous channel units made by

Phillips and the EMR division of Weston Instruments, and

the magnetic "strip" multiplier made by Bendix, as well as

the discrete dynode multipliers made by EMI, RCA, EMR,

Nuclide Analysis Associates, and others.

6. ELECTRONICS FOR LABORATORY TIME-OF-FLIGHT STUDIES

The electronic requirements for laboratory TOF studies and for actual flight experiments are similar, but the specific electrical equipment used in the laboratory and aboard a satellite is necessarily quite different. In this section the laboratory electronics system is described; a breadboard system for flight application is discussed in Section 7.

6.1 BASIC OPERATION OF THE SYSTEM

Recall that in the TOF method, gas from an external source (or reflected from some test surface) passes through a pulsed electron gun. During the electron gun current pulse, some molecules are excited to metastable states. The resulting packet of metastable molecules spreads out in time; the excited molecules reach the detector after time intervals which are inversly proportional to their velocities.

The system shown in Fig. 6.1 performs the following functions during the acquisition of time-of-flight data:

(1) It supplies short, periodic pulses to the electron gun in order to excite the molecules;

(2) It amplifies and shapes pulses from the detector;

(3) It prevents the entry into the pulse height analyzer of detector signals (due to photons) which occur during the firing of the electron gun;

(4) It modulates the pulses from the detector so that their amplitudes are proportional to the time

42

ELECTRON GUN

DETECTOR

PULSER

PREAMP
AMP
INT DISC

PULSER

INTEGRAL
DISC

GATE LINEAR GATE
DISABLE MODE

WAVEFORM
GENERATOR

LINEAR GATE 2
ENABLE MODE

RC SHAPING
AMPLIFER

MULT.CHANNEL
PULSE HEIGHT
ANALYZER
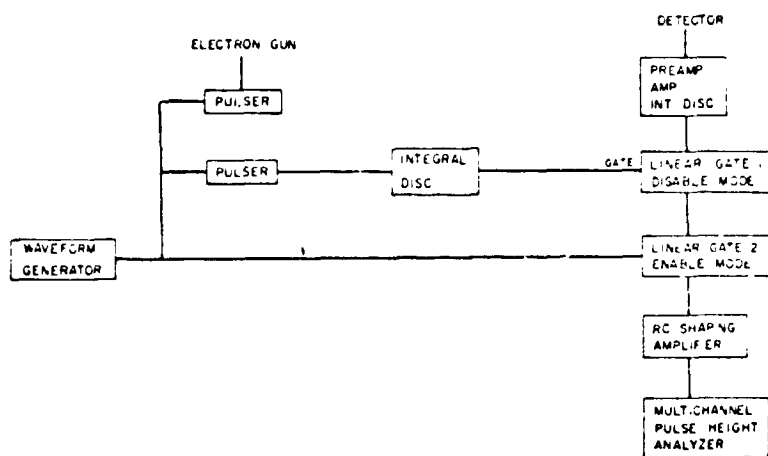
Figure 6.1   Block diagram of the time-of-flight electronics.

> intervals between the firing of the electron gun
> and the instants when the metastable molecules
> arrive at the detector;

(5)   It analyzes and stores these modulated pulses.
The cyclic operation of the TOF system is controlled by a
waveform generator which initiates operations for the
performance of functions 1, 3, 4.

Metastable molecules are produced by electron bombardment
in a field free region of the electron gun anode. A high
current pulse generator controls the electron gun anode
voltage. The pulses are typically 5-50 µsec wide and range
up to 100 volts in amplitude; their repetition rate is typically
1KHz. In order to remove detector pulses caused by photons
which are emitted during the electron gun current pulse, a
linear gate operating in the disabling mode is employed. The

43

detector pulses are sent to the signal input of the linear gate; a gating pulse, adjusted to occur simultaneously with the electron gun pulse, is sent to the gate input of the linear gate. Any detector pulses occuring during this gating interval are not passed.

Time-to-pulse-height conversion is achieved with the use of a second linear gate. A linear ramp is applied to the signal input of the gate; the detector pulses are applied to the gate input. Small portions of the ramp (width about 2 μsec) are passed when the detector pulses open the linear gate. The amplitudes of these portions are directly proportional to the time intervals between the firing of the electron gun and the instants when the metastable atoms arrive at the detector. Typical pulses are shown in Figure 6.2.

6.2 CIRCUIT DESCRIPTIONS

We obtain TOF spectra from more than one experimental system, and it is convenient for each setup to have as much of the electronic equipment continuously available as possible. Consequently, we have developed a simple, inexpensive and easily duplicated system to perform functions 1)-4) above. A block diagram of the system, similar to that shown in Figure 6.1, is shown in Figure 6.3. The basic operation is essentially that described above. The ramp generator determines the time base. The pulser for the electron gun supplies the necessary anode voltage control. The electron gun pulse is adjustable in time relative to the beginning of a sawtooth

44

SIGNAL INPUT
GATE I

GATE INPUT
GATE I

OUTPUT GATE I
AND
GATE INPUT
GATE 2

SIGNAL INPUT
GATE 2

OUTPUT
GATE 2
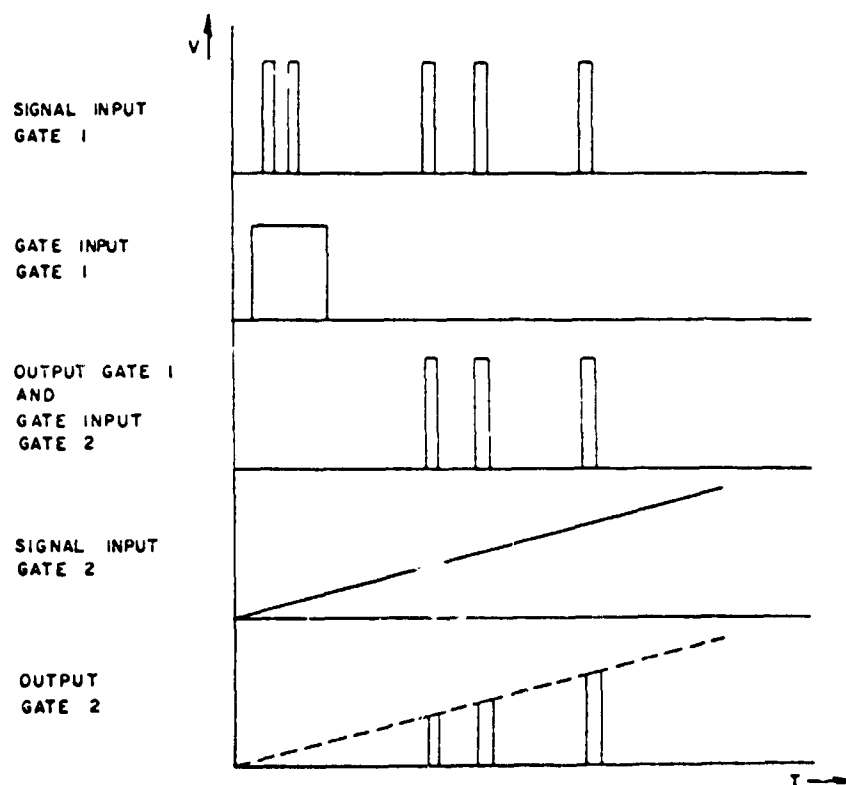
Figure 6.2 Typical pulse distributions, demonstrating
the functions of the linear gates 1 and 2 shown in Figure 6.1.

ELECTRON GUN

ELECTRON
GUN
DRIVER

DETECTOR

AMPLIFIER

LEVEL
CROSSING
DETECTOR

MONOSTABLE
MULTIVIBRATOR

INTEGRAL
DISC

LEVEL
CROSSING
DETECTOR

MONOSTABLE
MULTIVIBRATOR

GATE

DISABLE
GATE

GATE

LINEAR
RAMP
GENERATOR

ENABLE
GATE

TO PULSE
HEIGHT ANALYZER
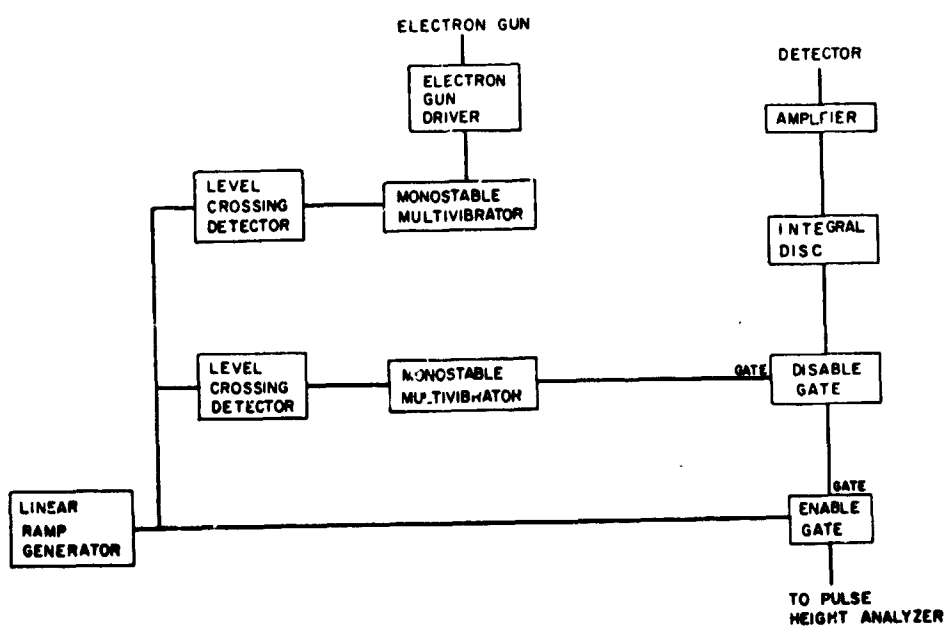
Figure 6.3 Block diagram of the laboratory time-of-flight
electronics.

45

cycle by biasing a level crossing detector; in width by
adjusting a variable resistor in the monostable multivibrator;
and in magnitude by a voltage externally applied to the electron
gun driver. The control to the disable gate (to block photons)
is derived from a level crossing detector and monostable
multivibrator identical to those used for the electron gun.
Time-to-pulse-height conversion is achieved in an identical
manner to that described above. The system we have constructed
to perform functions 1)-4) above contains about $65 worth of
semiconductor components. Brief descriptions and circuit
diagrams of some of the constructed circuits follow.

6.2.1 The Sawtooth Generator

The sawtooth generator is an integrator driven by a
modified Schmitt trigger and a buffer. The trigger controls
the integrator by reversing the charging current when the
appropriate integrator output levels are reached. R_1, R_2 and
R_3 determine the trigger levels (in our case 0 and 8 V). The
variable resistor then determines the slope of the sawtooth.
The capacitor is charged through an operational amplifier
for improved linearity.
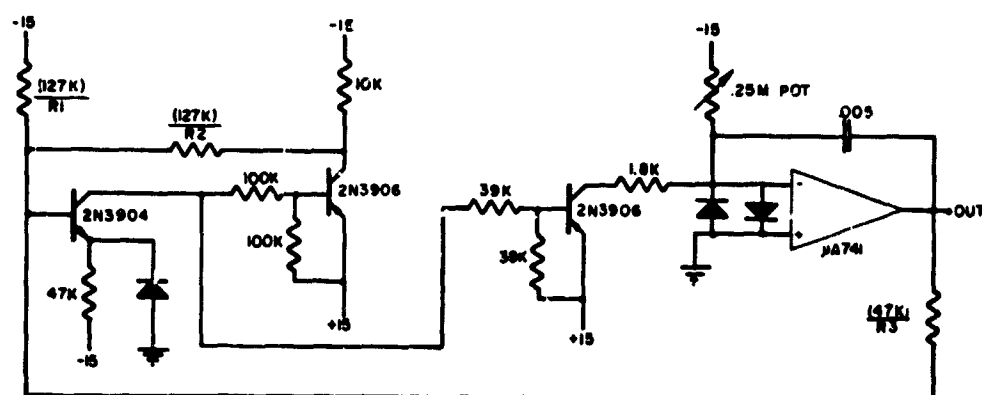
Figure 6.4 Sawtooth Generator.

46

6.2.2 The Level Crossing Detector

The level crossing detector is composed of a differential comparator, a differentiating network and an inverting amplifier. The sawtooth triggers the comparator at some adjustable voltage level. The output voltage of the comparator is positive (~9 V) until it is triggered; it then drops to a less positive voltage (~4 V) until the end of the cycle. This square pulse is differentiated and fed to the base of a transistor which is heavily conducting. The positive pulse cannot turn the transistor on further so it does not appear at the collector. The negative pulse shuts off the transistor, giving a positive pulse out.
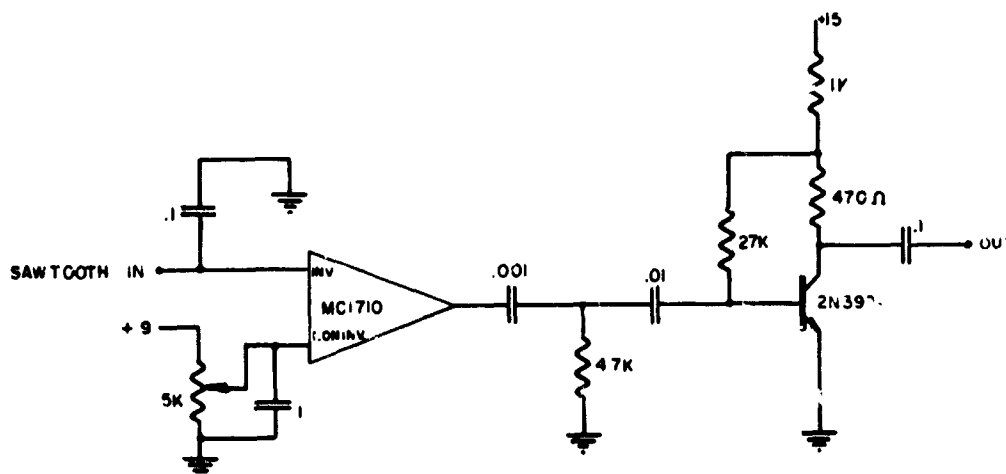
Figure 6.5 Level Crossing Detector.

47

6.2.3 The Monostable Multivibrator

The monostable multivibrator unit consists of a
trigger isolater, a multivibrator proper, and an inverting
amplifier. The duration of the output pulse is controlled by
a 50 K potentiometer used as a variable resistor. The integral
discriminator is identical to the multivibrator except for a
fixed resistor to make the output pulse 2 μsec in duration and
a varible offset bias applied to the input transistor base.
This biasing serves as the threshold control of the integral
discriminator.
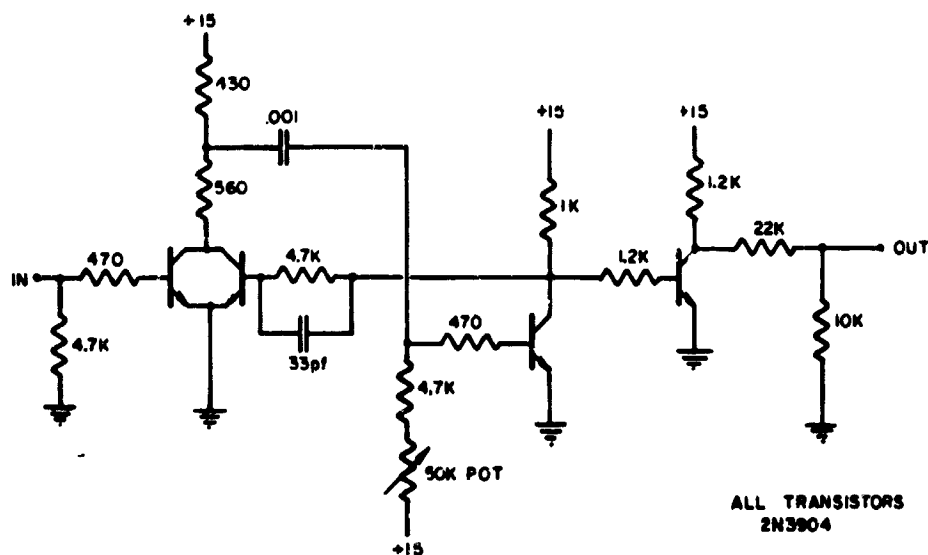
Figure 6.6 Monostable Multivibrator.

48

6.2.4 The Linear Gates

The enable and disable gate circuits each use a
single field effect transistor. In the enabling gate, the FET
normally has a low resistance compared to the 100 K resistor
so the output is grounded. The gate pulse gives the FET a high
resistance and then most of the signal appears across the 100 K
at the output. In the disable gate however, the FET is in
series and normally passes the signal. The gating pulse makes
the FET a high impedance relative to the 30 K and effectively
grounds the output.
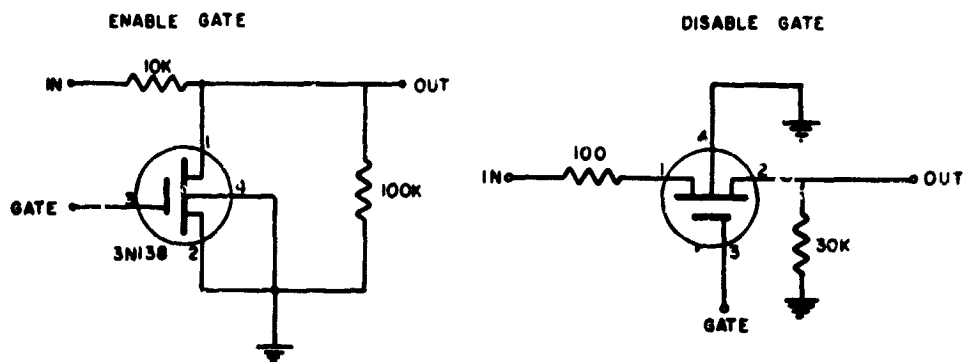
Figure 6.7 Linear Gates.

49

7. BREADBOARD ELECTRONICS FOR A FLIGHT EXPERIMENT

An analysis of the electronic system required to support a flight experiment indicated that two developments were needed: 1) a data processor to perform the time-of-flight analysis, and 2) an electron gun which would both meet the experimental needs and be flyable from the point of view of ruggedness and power. The breadboard development effort was concentrated in these two areas. The necessary technology for constructing the remaining subsystems (principally power supplies) is considered to be adequately developed.

7.1 THE DATA PROCESSOR

The optimum choice of the data processor for a time-of-flight analysis depends in a direct way on the telemetry data rate available to the experiment. The choices range from telemetering the time of flight of each metastable detected, to telemetering the total number of pulses arriving during pre-selected time increments over preset integration times. The advantages of the first choice are simplicity and flexibility at the expense of data rate, while the advantage of the second is low data rate at the expense of increased complexity and the need to define a priori integration times. The system that has been designed and built is a non-integrating type which can be directly expanded to an inflight integrating system with the addition of "off the shelf" hardware. In addition, the analyzer is designed to provide either digital or analog outputs to adapt to satellite requirements.

The basic system consists of a pulse amplifier, a dis-
criminator, a 200 KHz clock driving seven flip flops in
series, and an electron gun driver. The 2^7 output states of
the flip flops provide a 128 channel time code which incre-
ments every five microseconds. At the beginning of each
frame, i.e., at the negative going change of state of the
most significant bit, the electron gun driver is pulsed.
Each data pulse received at the electron multiplier is then
conditioned by the pulse amplifier and discriminator, and
used to gate the time code into the associated output cir-
cuitry. Therefore, each time code word received indicates the
elapsed time between that data pulse and the preceding
electron gun pulse. Figure 7.1 is a block diagram of this
basic system.

The system is straightforward, the only subtle innovation
being the addition of a pulse stretching circuit. Since
transition times for the flip-flop states make up about 5%
of the frame time, and this transition time is essentially
noise, it is desirable to keep data pulses from gating time
code words during the transitions. To do this the properties
of the discriminator are utilized; the discriminator is a
Schmitt trigger which is turned on when the input pulse
exceeds the upper trigger level and is not turned off until
the input falls below the lower trigger level. Each time the
least significant flip flop changes state a pulse slightly
longer than the transition time of all seven flip flops is
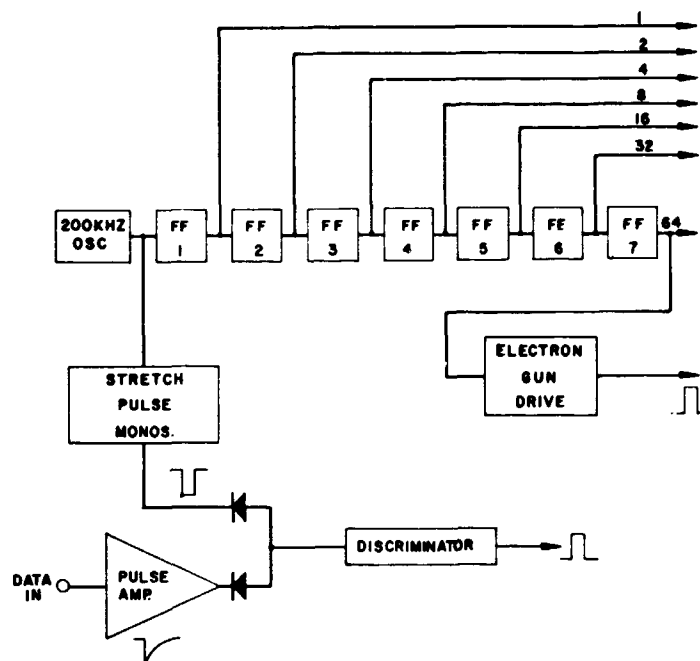generated and fed to the discriminator through a diode OR

Figure 7.1 Basic time-of-flight analyzer system.
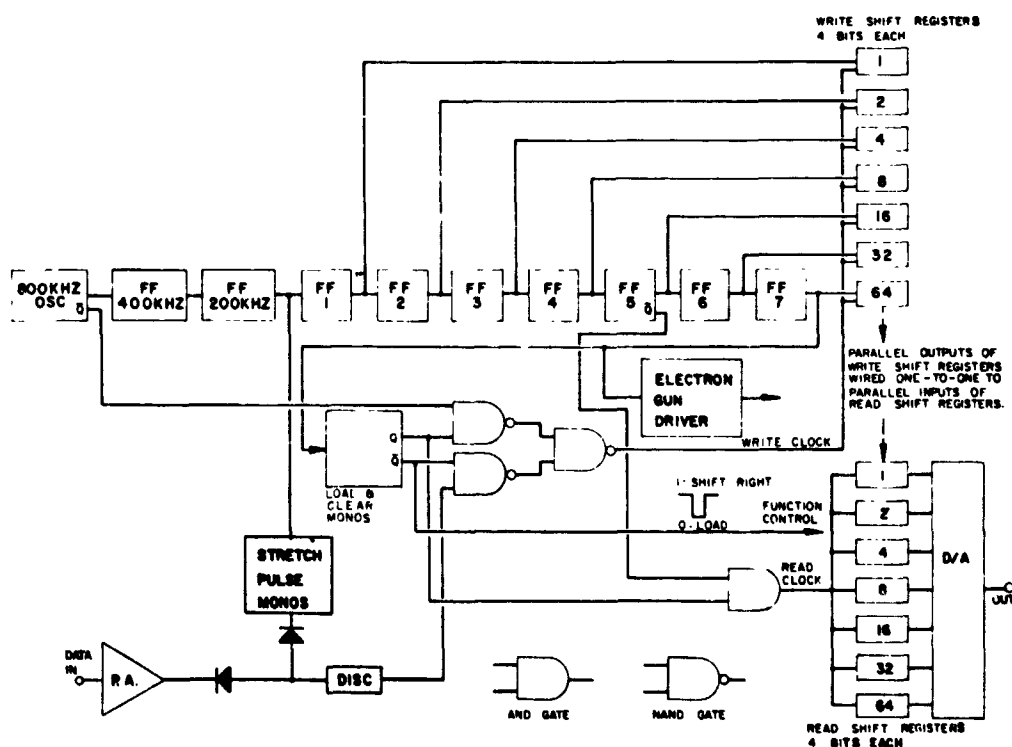
Figure 7.2 Non-integrating, analog output time-of-flight analyzer.

gate along with the data input. The amplitude of the stretch pulse is set between the trigger levels such that, if no data pulse is present above the upper trigger level, the discriminator is not triggered. However, once the discriminator is triggered by a data pulse it cannot turn off until the stretch pulse disaprears, thus prohibiting discriminator output pulses from falling during the transitions (in this system falling edges initiate triggering).

To illustrate one of many possible output circuits that can be added to the basic system, a non-integrating analog output system is described. This arrangement is similar to one that was constructed and tested at the Space Physics Research Laboratory in breadboard form. Referring to the block diagram in Figure 7.2, the additions consist mainly of a set of READ and WRITE shift registers and a D/A converter. The time code is gated by the data pulses into the WRITE shift registers and stored until the beginning of the next frame. At the beginning of each frame the contents of the WRITE shift registers are first dumped into the READ shift registers; the WRITE registers are then cleared in preparation for the next data. Then as the WRITE shift registers store the randomly arriving data, the READ shift registers read the transferred data into the D/A converter at a periodic rate. This is done to reduce the telemetering bandwidth requirements from those required for random data. The necessary capacity of the shift registers for a satellite experiment is discussed in Section 9.1; for the breadboard system, however, it was found that four bits per register were adequate to insure

53

"infrequent" overflow. The timing functions are illustrated
in Figure 7.3.

The analog output data can be conveniently sorted, inte-
grated and displayed using a commercial pulse height analyzer.
The upper display in Figure 7.4 shows data taken by the
breadboard time-of-flight analyzer which have been sorted and
integrated as mentioned above; the lower display was produced
by the commercial analyzer and the laboratory electronics
(Section 6) under the same experimental conditions. The
vertical and horizontal scales were adjusted to be approxi-
mately the same.

To convert the system to a pulse code modulated (PCM)
output, the D/A converter is removed, the READ shift registers
are wired in series, and the READ clock rate is increased by
a factor of seven or more to shift out all twenty-eight bits
within the frame time. The output appears as non-return-to-
zero (NRZ) serial PCM.

A way to obtain integrated digitial data is to remove the
shift registers and feed the flip flop outputs to a binary-to-
decimal converter for sorting. Each decimal line of the con-
verter then drives a counter of the desired capacity to
provide a straightforward method of integration; substituting
a commercial memory for the counters would probably provide
more storage capability for a given volume. Addition of a D/A
converter to this system alters the integrating digital system
to an integrating system with analog output.
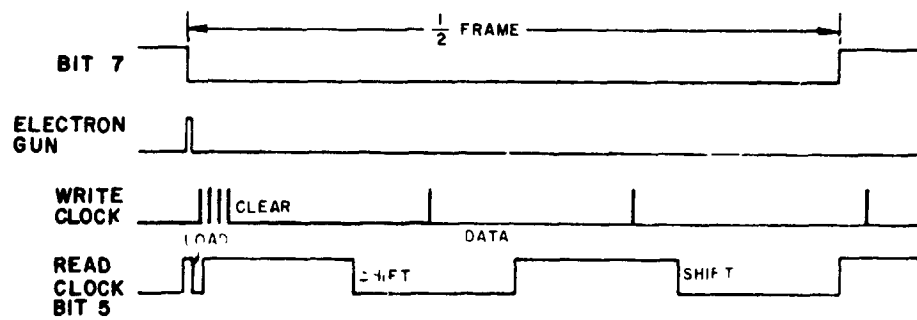
MAJOR TIMING FUNCTIONS
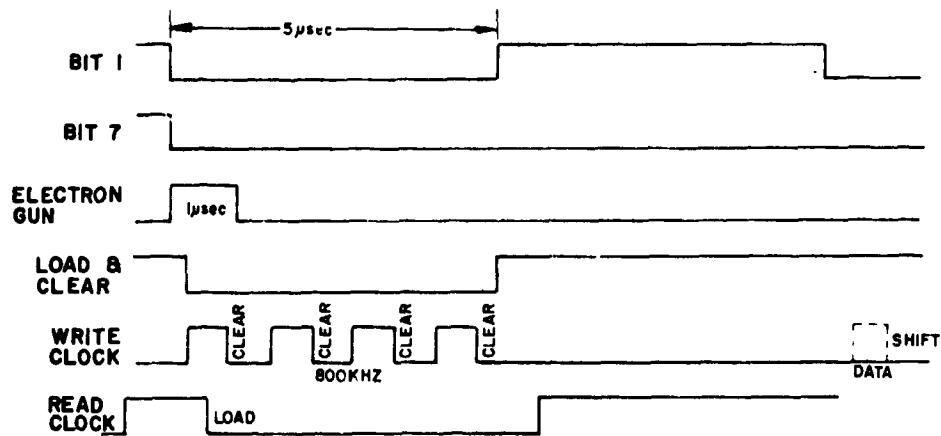
EXPANDED TIMING FOR LOAD AND CLEAR

Figure 7.3   Timing sequences.

55

Figure 7.4 Time-of-flight analyzer displays. Curve A shows data processed by the prototype satellite experiment electronics; curve B shows data processed by the laboratory electronics. Both displays are taken from oscilloscope displays from a commercial pulse height analyzer which was used for data storage; the distinctive steps in the curves are due to the 2-digit decoding used in the analyzer display.

7.2 THE ELECTRON GUN

In order to provide a suitably large burst of metastable molecules, the electron gun should produce a beam current of at least 5 mA at an accelerating voltage of 40 volts, and should have a planar beam geometry. The required engineering features are ruggedness, low power consumption, and immunity to atmospheric contamination when the cathode is cool. A planar Pierce gun with an impregnated matrix cathode seems to best satisfy the above conditions (Kirstein et al., 1967). Section 7.2.1 describes the design of the gun and Section 7.2.2 includes the test results and conclusions.

7.2.1 Design

The desired beam parameters are:

Beam current: 5 mA

Accelerating voltage: 40 volts

Beam shape: planar: thickness $2t$ = 2mm, length L = 10mm, width w = 10mm. A sectional view of a planar Pierce gun capable of approximating the desired beam shape is shown in Figure 7.5.

Define the following quantities:

$$P = \text{perveance} = I/V^{3/2}$$

$$N = \text{number of squares} = \frac{w}{2t}$$

$$P_{sq} = \text{perveance per square} = P/N$$

57
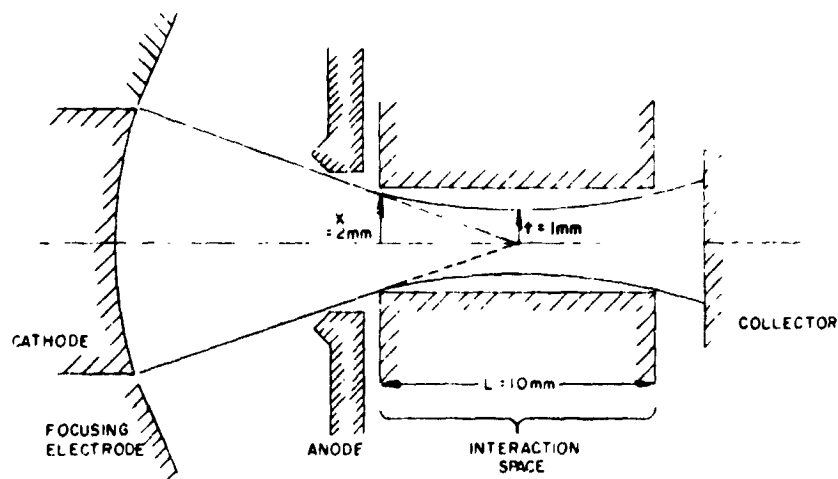
Figure 7.5   The planar Pierce gun.

For maximum perveance, i.e., maximum beam current, the
electrons must be aimed for the center of the interaction
space, as shown by the dashed lines in the figure.   Space
charge effects, however, will only allow the beam to reach
a minimum thickness of 2t.   The minimum thickness is related
to the thickness at the entrance of the interaction space by

$$\frac{x}{t} = 2.0$$

For such a gun the limiting perveance per square is given by

$$P_{sq} = 4\epsilon_o \sqrt{\frac{2e}{m}} \left(\frac{x}{L}\right)^2$$

$$= 21 \times 10^{-6} \left(\frac{x}{L}\right)^2 \text{ perv/square}$$

58

Using the given parameters ($x = 2$ mm and $L = 10$ mm) it is found that

$$P_{sq} = 0.84 \times 10^{-6} \text{ perv/square}$$

In addition, the number of squares desired is

$$N = \frac{w}{2t} = 5$$

so that

$$P = 4.2 \times 10^{-6} \text{ perv.}$$

At 40 volts and the given perveance, the maximum beam current is only 1.06 ma. Thus, to increase the current at 40 volts, it is necessary to employ a focusing magnet.

Consider a magnetic focusing field $\overline{B}$ in the direction of the electron flow (see Figure 7.6). Let v_o be the velocity of the beam electrons the x-direction. Under conditions of Brillouin flow the solution to the differential equation of motion is

$$\frac{2e}{m} q(y) = v_o^2 + \omega y^2$$

where q is the stream potential and

$$\omega = \frac{eB}{m}$$

In addition, the presence of the magnetic field introduces a shearing motion in the plane of the beam, as indicated in Figure 7.6. The resulting lateral velocity of the electrons
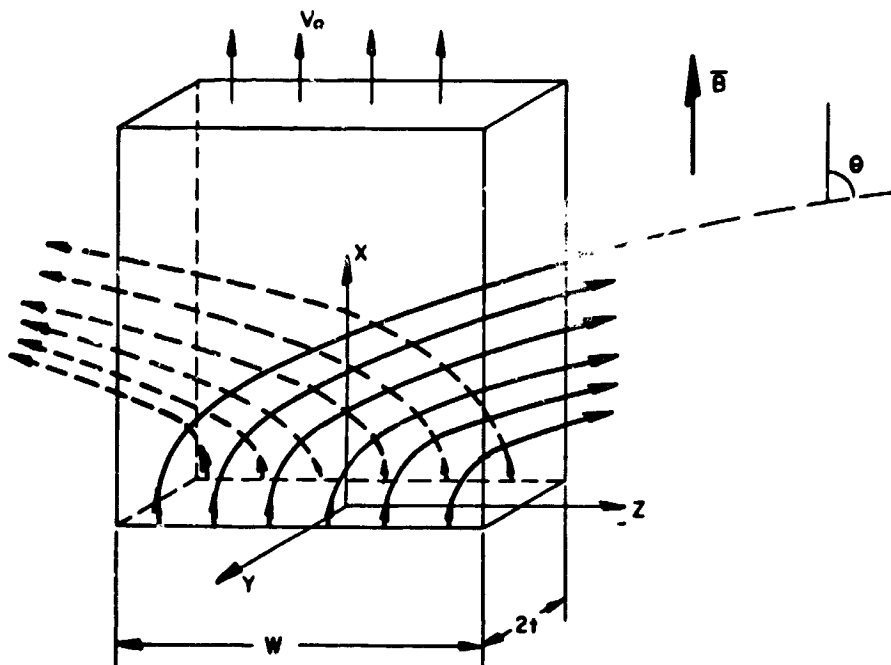
Figure 7.6 Idealized electron beam with magnetic focusing.

is found to be

$$\dot{z} = \omega y$$

Introducing the total electron velocity v, it is easily shown that

$$\frac{\dot{z}}{v} = \frac{\alpha}{1 + \alpha^2}$$

where

$$\alpha = \frac{\omega y}{v_o} = \tan \theta$$

and θ is the angle the total velocity vector makes with the

60

desired direction of flow (the x-direction).

For this flow the maximum perveance per square is found to be

$$P_{sq} = 2 \epsilon_o \sqrt{\frac{2e}{m}} \; \alpha^2$$

$$= 10.5 \times 10^{-6} \; \alpha^2 \; \text{perv/square}$$

For a 5 mA beam at 40 volts, the definition of perveance gives $P = 19.8 \times 10^{-6}$ perv. Consequently

$$P_{sq} = \frac{19.8 \times 10^{-6}}{5} = 3.96 \times 10^{-6} \; \text{perv/square}$$

Using the previous equation, this leads to

$$\alpha^2 = \frac{3.96}{10.5} = .377$$

or

$$\alpha = .614$$

With this value of α, the minimum strength of the confining magnetic field can be calculated

$$B_{min} = \frac{m\omega}{e} = \frac{m\alpha v_o}{e\underline{y}}$$

$$= 131 \; \text{gauss}$$

For a smaller field than this, it is not possible to obtain 5 mA at 40 volts.

The shearing angle at the surface of the electron sheet can also be evaluated. From the definition of α, the lateral velocity of the electrons at the beam surface is 61.4% of the

axial velocity, leading to a shearing angle

$$\theta = \arctan \alpha = 31.5°$$

Ideally one would like as large an electron current as possible. However, increasing the gun current requires higher perveance, which increases the shearing angle. Unfortunately, it is desirable to keep this angle as small as possible, since a large range of angles complicates the analysis of the velocity distribution of the gas particles.

7.2.2 Testing and Results

An electron gun was constructed to the specifications of the previous Section (see Figure 7.7). Figure 7.8 shows the electron gun and collector plates mounted inside a bell jar. An overall view of the entire test system is shown in Figure 7.9.

The electron gun collector used in the test consists of two molybdenum plates, one inch in diameter, coated with a graphite paint to reduce electron reflection and secondary emission. The plates are insulated from each other and spaced 0.05 inch apart. A 0.012 inch diameter hole was drilled in the center of the collection plate nearest the anode. This hole allows a small fraction of the beam current to reach the second collector plate; by measuring the current to the second collector as a function of the position of the double collector assembly with respect to the remainder of the gun, it is possible to determine the relative current density over the cross section of the beam.

.OOI-.OO2 MOLYBDENUM SHIELD
.OI4 GAP BETWEEN SHIELD & CATHODE
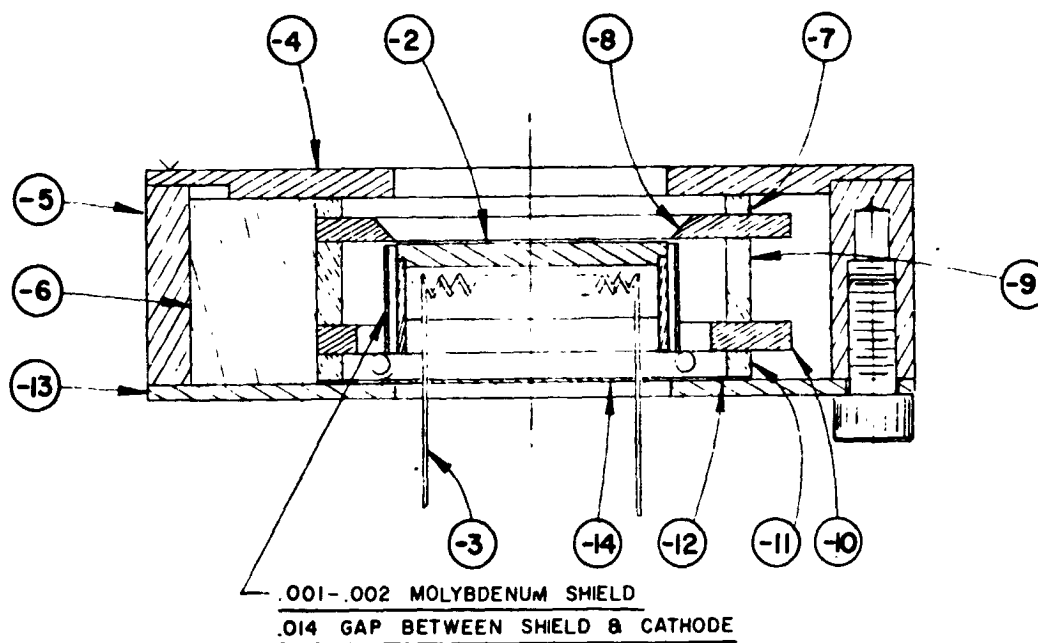
2. CATHODE
3. FILAMENT
4. ANODE (1.125" D)
5. ANODE CYLINDER
6. ALIGNMENT ROD
7. ANODE-FOCUS ELECTRODE SPACER
8. FOCUS ELECTRODE
9. CATHODE-FOCUS ELECTRODE SPACER
10. CATHODE SUPPORT DISC
11. END PLATE-CATHODE SPACER
12. SPRING
13. END PLATE
14. HEAT SHIELD

Figure 7.7 Design drawing for electron gun.

63

Figure 7.8   The electron gun mounted for testing.

Figure 7.9   The electron beam analyzer.

Test results are presented in the form of graphs
as follows. A current density profile of the electron beam
is shown in Figure 7.10. In Figure 7.11 the accelerating
voltage (anode voltage) is held constant at 40 volts and the
electrode currents are plotted as a function of collector
voltage. Figure 7.12 is a graph of the electrode currents
versus accelerating voltage, where the collector voltage is
held equal to the accelerating voltage. In Figure 7.13 the
accelerating voltage is constant at 40 volts, the focus elec-
trode voltage is varied and the electrode currents are re-
corded. Figure 7.14 is similar to Figure 7.13 except the
accelerating voltage is 20 volts. Figure 7.15 is a plot of
the filament current versus filament voltage. In each case
the magnetic field intensity is 245 gauss, a value larger
than that indicated by the design calculations.

7.2.3 Conclusions

Operating data obtained for the electron gun are
shown in Table 7.I. Higher beam currents are obtainable using
cathode temperatures above that recommended for operation by
the manufacturer, and at the expense of larger focus elec-
trode currents. At the recommended operating temperature
the cathode power consumption is 11 watts. It was also found
that the 5 mil tungsten cathode leads are easily fractured
in spite of their 3% rhenium content.

In view of the above factors it is felt that
although the electron gun is useful as it stands, improvement
for flight applications is desirable in the areas of rugged-
ness and power consumption.

65
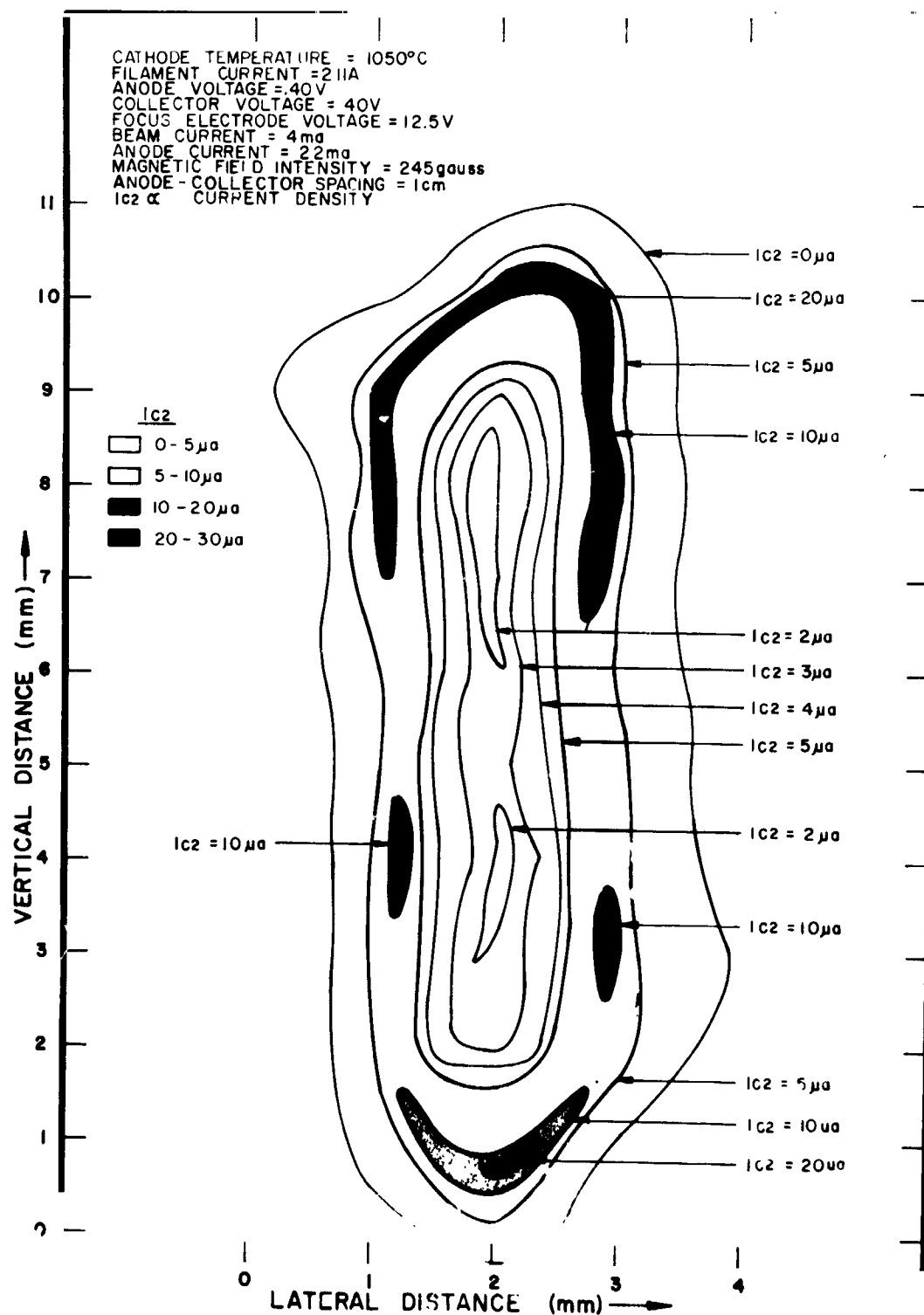
Figure 7.10 Relative cross sectional current density at the anode for an anode-collector spacing of 1 cm.
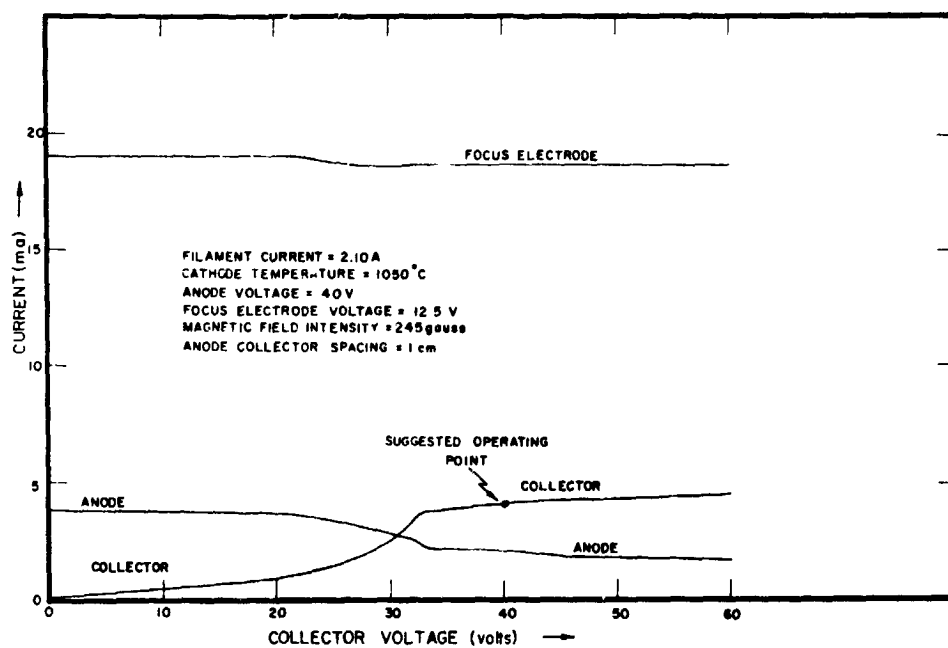
Figure 7.11   Electrode currents vs. collector
voltage for fixed anode voltage.
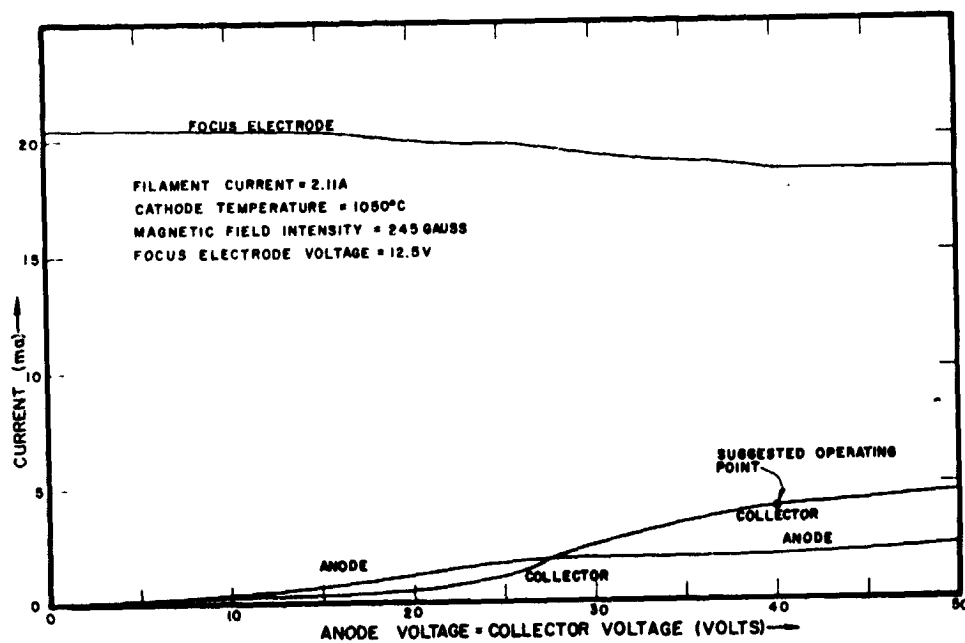
Figure 7.12   Electrode currents vs. accelerating voltage.

CATHODE TEMPERATURE = 1050 °C
FILAMENT CURRENT = 2.10 A
MAGNETIC FIELD INTENSITY = 245 gauss
ANODE VOLTAGE = 40 V
COLLECTOR VOLTAGE = 40 V
ANODE - COLLECTOR SPACING = 1 cm

FOCUS ELECTRODE

COLLECTOR

ANODE

CURRENT (ma) ——→

FOCUS ELECTRODE VOLTAGE (volts) ——→
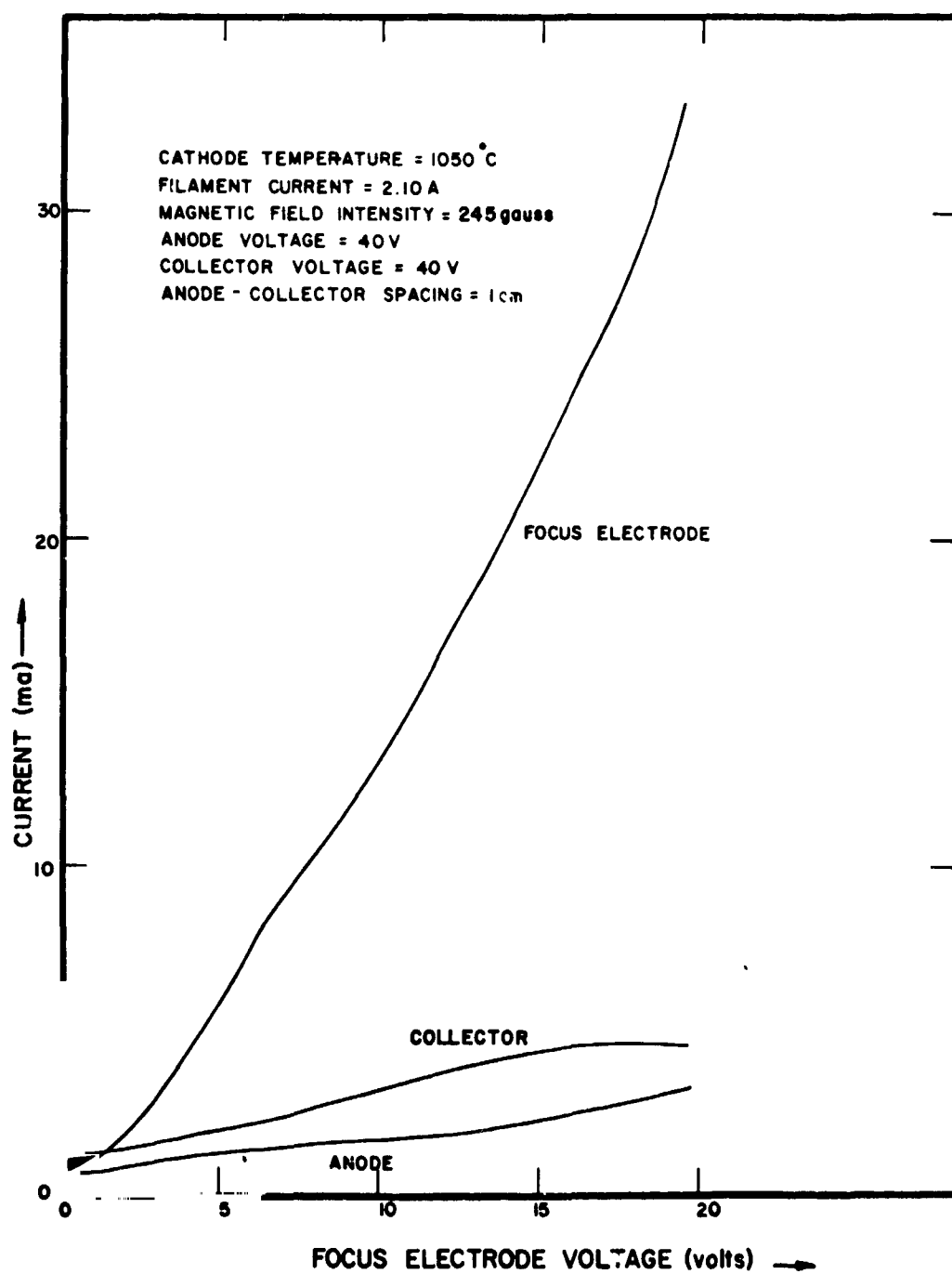
Figure 7.13 Electrode currents vs. focus electrode voltage;
anode voltage = collector voltage = 40 v.

68

CATHODE TEMPERATURE = 1050°C
FILAMENT CURRENT = 2.10 A
MAGNETIC FIELD INTENSITY = 245 gauss
ANODE VOLTAGE = 20 V
COLLECTOR VOLTAGE = 20 V
ANODE - COLLECTOR SPACING = 1 cm

FOCUS ELECTRODE

ANODE

COLLECTOR

CURRENT (ma) →

FOCUS ELECTRODE VOLTAGE (volts) →
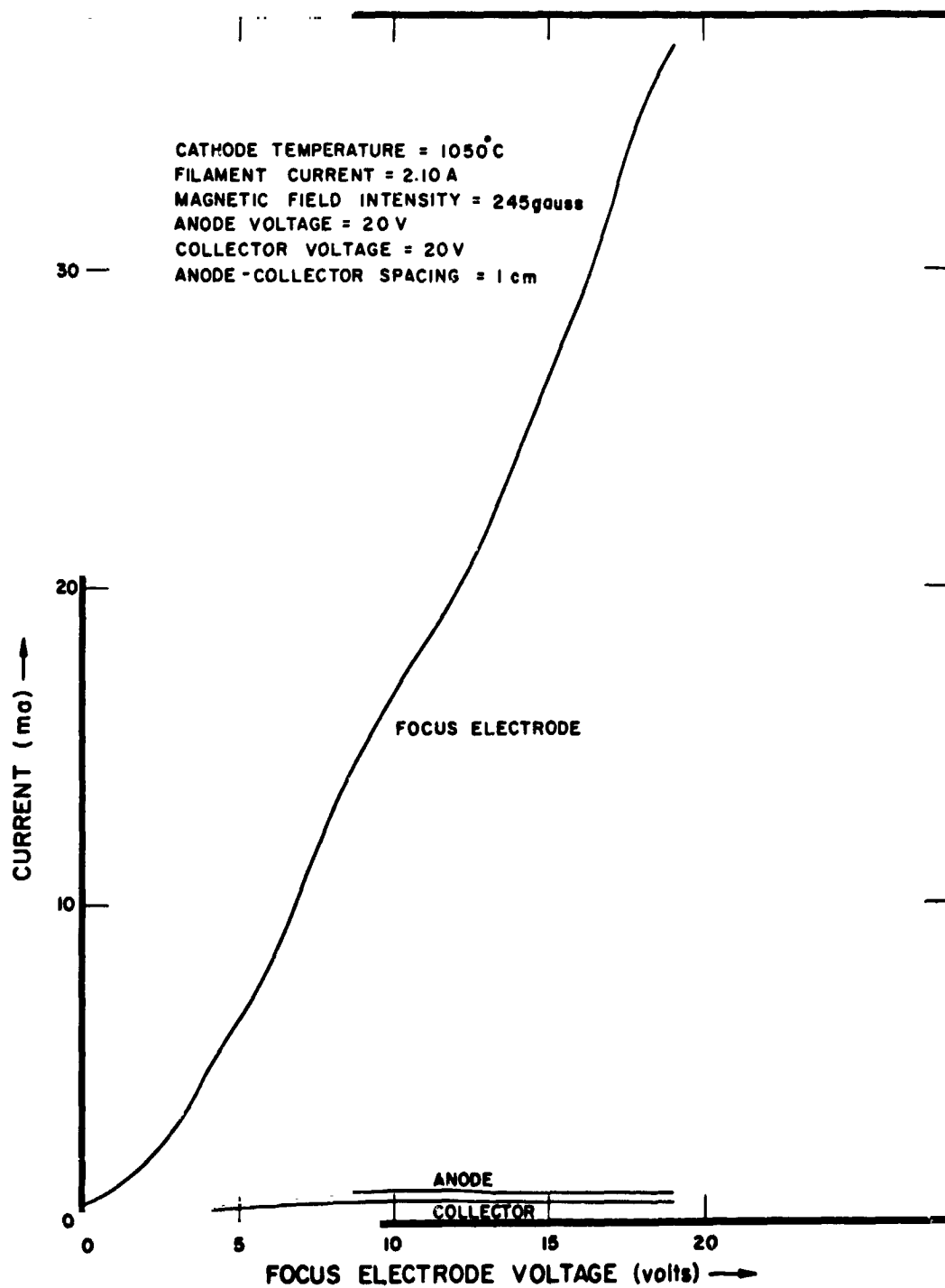
Figure 7.14 Electrode currents vs. focus electrode voltage;
anode voltage = collector voltage = 20 v.

69
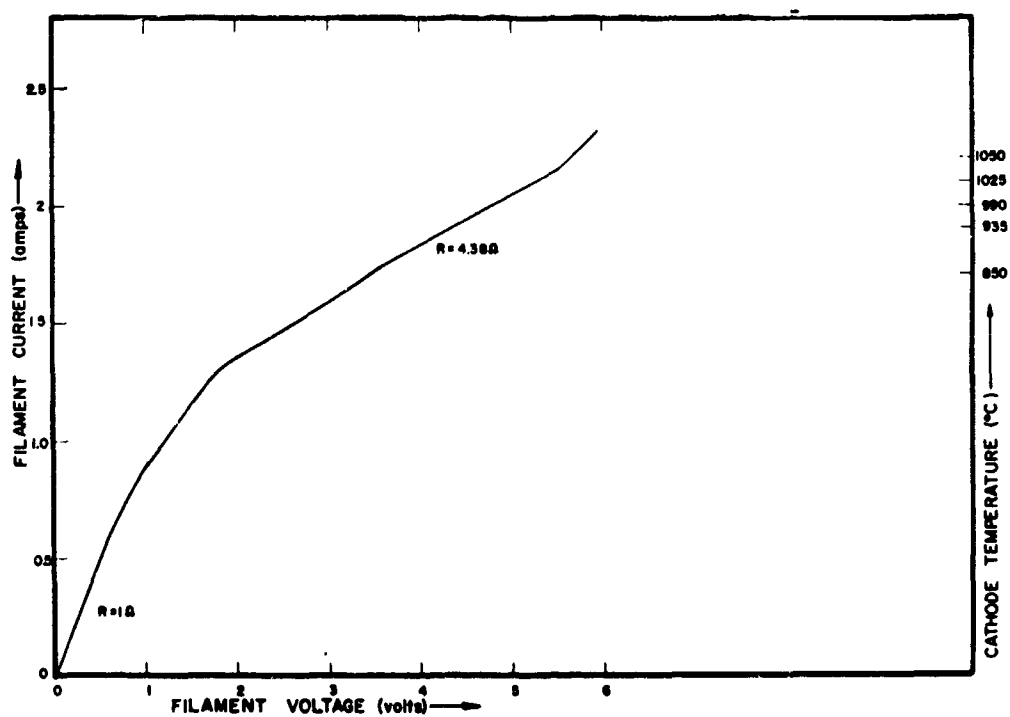
Figure 7.15 Filament current vs. filament voltage
vs. cathode temperature.

Anode & Collector Voltage	Collector Current Ma	Anode Current Ma	Focus Electrode Voltage	Focus Electrode Current Ma
10	.3	.3	1.9	2.2
20	1.0	9	7.5	8.0
30	2.4	1.8	12.5	20.5
40	4.0	2.2	12.5	20.5

I_F = 2.1 amps   B = 245 Gauss

Table 7.I   Operating Parameters for the

Electron Gun

8.   MOLECULAR FLUX ESTIMATES

In order to provide convenient numerical data on conditions encountered by a flight experiment, particle fluxes have been compiled, using a standard atmosphere; these are shown graphically in Figures 8.1 and 8.2 (Zorn and Pearl, 1967). The fluxes (N_2, O_2, 0 and the totals) are for the previously proposed ODYSSEY orbit with an apogee of 2,000 km and a perigee of 200 km.   Satellite altitude and time from perigee are also indicated.   All atmospheric parameters have been taken from the CIRA 1965 reference atmosphere, Model 4.

Figure 8.1 has been drawn using parameters for 0400 hours; Figure 8.2 has been drawn using parameters for 1400 hours. Consequently, the two sets of data provide results for the extreme diurnal exospheric temperatures encountered during one equatorial orbit.
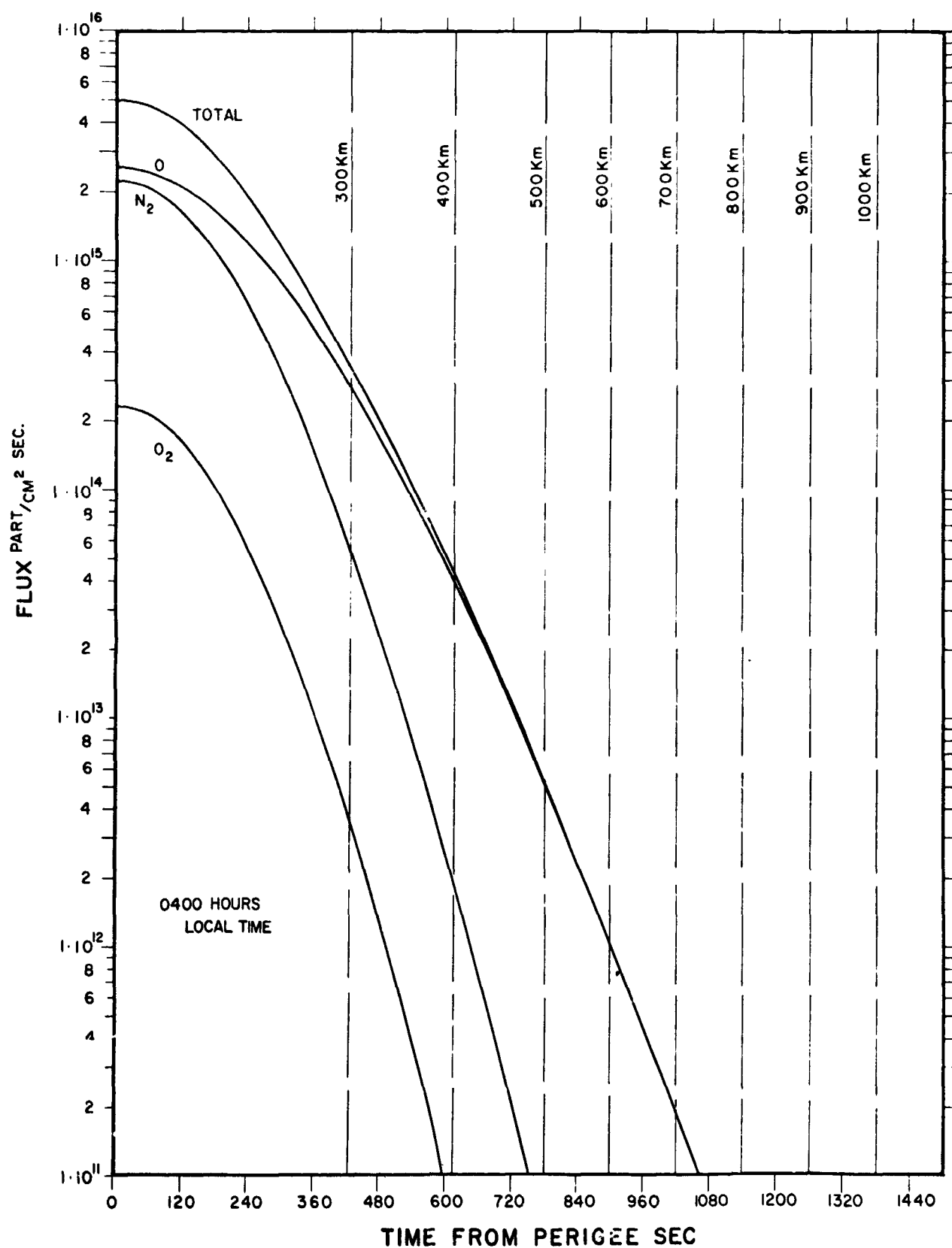
Fig. 8.1 Fluxes of major atmospheric constituents to a satellite in proposed ODYSSEY orbit for 0400 hours local time.
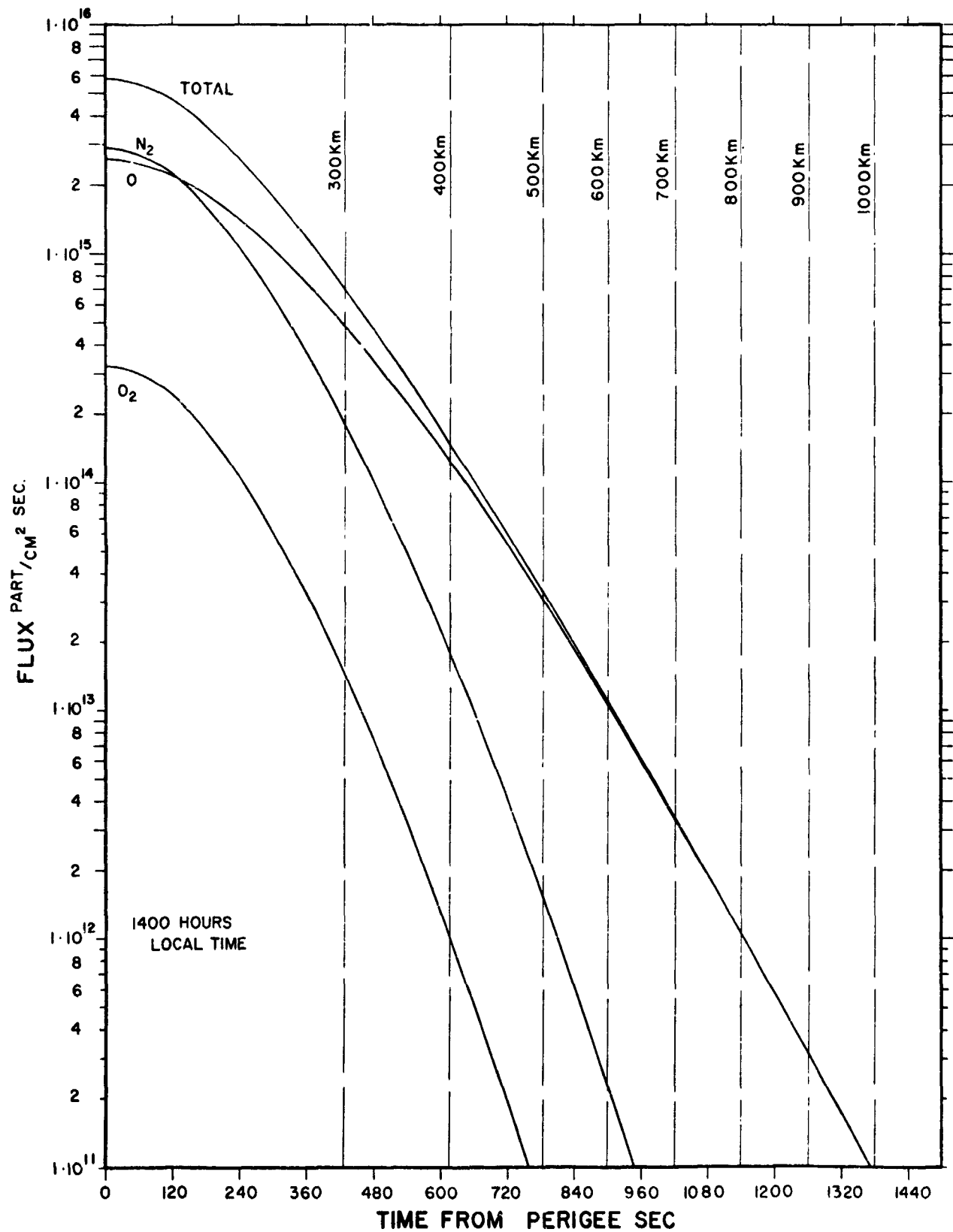
Fig. 8.2 Fluxes of major atmospheric constituents to a
satellite in proposed ODYSSEY orbit for 1400 hours local time.

9. ENGINEERING PARAMETERS OF THE FLIGHT EXPERIMENT

A wide range in the possible scope of an in-flight gas-surface interaction experiment exists. An initial experiment, for example, might involve a time-of-flight analysis of ambient molecular nitrogen, taken for a single incident and reflected angle. A simple experiment of this type could be carried out on a rocket for reasonable cost and would require only modest weight, power, and telemetry rate.

A "full blown" version of the experiment, on the other hand, would be costly in terms of volume and data rate, and would require a rather special satellite system on which to mount it. The financial cost of such an experiment would also be great and would clearly dictate the first step precursor. On the basis of that rationale, the engineering parameters of the simple version are presented below, and the parameters of a more complex experiment are discussed only in a general way.

9.1 TELEMETRY REQUIREMENTS

The breadboard electronic system which has been built provides 128 time channels (seven binary bits of information) and can accomodate up to 4 pulses per frame. Using time code increments of five microseconds requires operating at a repetition rate of $\frac{1}{128 \times 5 \times 10^{-6}}$ = 1560 frames per second; with no inflight integration this would require a data rate of 44,000 bits/second per detector in the array (Figure 1.2).

This rate is reasonable for a rocket flight of a simple, single-surface experiment but would probably be prohibitive for a satellite utilizing a tape recorder, although a reduction in rate might be realized by making the system adaptive to the minimum information rate required for experiment resolution. OGO-6, for example, with 25 experiments provides only an 8,000 bit/second rate with full orbit coverage. Therefore, for a satellite, it would undoubtedly be necessary to integrate in flight. The integration time would be a strong function of the satellite orbit and of the scope of the experiment.

9.2 POWER, SIZE, AND WEIGHT REQUIREMENTS

The power required for the experiment is minimal. In its current state of development 15 watts would be adequate and it is anticipated that 10 watts can be easily achieved. A multiplicity of detector surfaces would raise this estimate only slightly since a major portion of the power is used by the electron gun, and need not be duplicated.

The volume required for the electronic system is .5 cubic feet. The volume and dimension of the analyzer system depends on the complexity of the experiment. A simple version could be mounted in .5 cubic feet or less for a total of 1 cubic foot and with a total weight of 20 pounds.

9.3 STABILIZATION REQUIREMENTS

It is desirable and perhaps essential for the experiment to maintain a constant angle to the velocity vector during

acquisition of any one set of data. In a rocket experiment, this criterion would be satisfied adequately in a stable rocket. For a satellite experiment, two axis stabilization would be desirable. An ideal condition would be a fully stabilized platform in a circular orbit at a low altitude.

9.4 SUMMARY OF ENGINEERING PARAMETERS FOR A SIMPLE GAS SURFACE INTERACTION EXPERIMENT

The major engineering parameters for a simple rocket-borne experiment are tabulated below:

Weight	20 pounds
Volume	1 cubic foot
Power	15 watts
Telemetry Rate	64 K bits/sec

Table 9.I Engineering Parameters.

10. SUMMARY AND CONCLUSIONS

10.1 SUMMARY

The metastable time-of-flight technique has been developed to the point where it can be used to perform gas-surface interaction measurements in situ in the earth's atmosphere. Much of this development has been performed under the present contract. The work includes the following:

A. The effect of recoil on the velocity distribution of metastable atoms or molecules produced by electron impact has been studied in detail (Section 2). It has been found that the velocity distributions can be significantly different from what would be expected if recoil effects were negligible. Given the conditions of a pulsed electron beam directed at right angles through a collimated beam of thermal energy helium atoms, it has been determined both experimentally and from kinematic arguments that the metastable velocity distribution has two peaks. In addition, both the peak separation and mean velocity of the distribution are sensitive to such parameters as electron energy and deflection angle. An understanding of this problem is essential for the correct analysis of data from any future flight experiments utilizing this technique.

B. The effect of short-lived metastable states on the interpretation of velocity distributions in N_2

78

beams has been studied (Section 3). In extracting

information about the velocity distribution of the

ground state beam from measurements on a metastable

beam, it is simplest to assume that the lifetime of

the metastable level is infinite. However, the

metastable $a^1\pi_g$ state of N_2 has a lifetime which

is comparable to the drift time of particles in

the proposed instrument.

The lifetime of this excited level, which must be known

in order to take proper account of the decay of

metastable molecules which occurs while the beam

drifts from the electron gun to the detector, can

be measured in two ways. The first, a time-of-

flight method, provides lifetime information by

comparing separate time-of-flight spectra obtained

using long-lived and short-lived states of metastable

molecules. The second method utilizes the decay of

the total metastable signal due to a single short-

lived component with distance. In the present work

the first method has been employed more successfully

than the second.

C. A time-of-flight system which is capable of observ-

ing a gas flux from a given direction is described in

Section 4. With a simple initial system an angular

resolution of better than 6° has been achieved. It

is essential to know the collimation of the incoming

beam for a correct description of recoil effects on velocity distributions (see Section 2). By using a directional gas analyzer, a time-of-flight system with the desired collimation for a given experiment can be designed.

D. The detection of metastable atoms and molecules using a continuous channel electron multiplier (Bendix Channeltron) is discussed in Section 5. Such detectors have been used to detect a wide range of metastable molecular species with excitation energies in excess of 6 eV. They appear promising as detectors for a satellite experiment.

E. The basic electronic system for acquiring laboratory time-of-flight data is discussed in Section 6. It utilizes time-to-pulse-height conversion and pulse height analysis.

Breadboard electronics for data analysis in flight experiments have been successfully tested in the laboratory and are discussed in Section 7. A prototype electron gun for satellite experiments has been designed; its operation is discussed in Section 7.

10.2 CONCLUSIONS AND RECOMMENDATIONS

The objective of this study has been to develop a technique and associated flight hardware for measuring the velocity distribution of molecules in a rarefied gas; the resulting experiment package is to be used for the measurements of gas-surface interaction phenomena in situ in the earth's atmosphere.

The metastable time-of-flight system described in this report has been prepared to achieve this objective. Specifically, it has been demonstrated that: a) the velocity distributions of metastable atoms produced by electron impact can be measured with a time-of-flight analyzer, and b) these distributions can be related to the incident gas flux through kinematic considerations. In addition, breadboard electronics for data analysis in flight experiments has been successfully tested in the laboratory. Thus the basis for the measurement has been established.

As a preliminary test of the above method, a simple experiment (see Section 9) could be carried out on a rocket. This would provide a verification of the total system.

APPENDIX I

EFFECT OF RECOIL ON THE VELOCITY DISTRIBUTION
OF METASTABLE ATOMS PRODUCED BY ELECTRON IMPACT *

J. C. PEARL, D. P. DONNELLY ana J. C. ZORN

Randall Laboratory of Physics, University of Michigan, Ann Arbor, Michigan 48104, USA

We have shown both experimentally and by a simple kinematic argument that the velocity distribution
in a beam of metastable atoms produced by electron bombardment of ground state atoms deviates strongly
from the velocity distribution of the ground state atoms.

The velocity distribution of metastable atoms often enters explicitly into the analysis of resonance
[1] and collision [2,3] experiments done with atomic beams. However, there have been few direct mea-
surements and no correct theoretical description of the velocity distribution in a beam of metastable
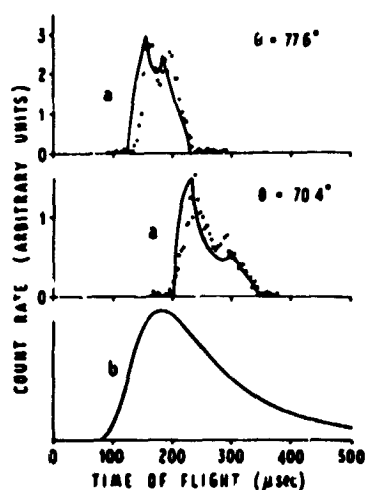
Fig. 1. Time-of-flight spectra for helium. Points represent experimental data. Curves a are theoretical accounting
for the angular divergence of the incoming, ground state beam, assuming $E - E^* - 0.75$ eV. Curve b is theoretical if
recoil effects are neglected.

atoms formed in the common experimental arrangement where ground state atoms in a collimated beam are excited by a transverse beam of electrons.

In our experiment a pulsed electron beam is directed at right angles ($\Phi = 90^0$) through a collimated beam of thermal energy helium atoms. The metastable atoms are detected [4] with an electron multiplier (Bendix Channeltron) which can be rotated about the interaction region in the plane defined by the incoming electron and atom beams. Samples of data taken at two different angles θ (angles measured from direction of electron beam) are plotted as points in fig. 1. Striking features of these results, when compared with what would be found if recoil effects were negligible (curve b in fig. 1) include the *narrowness* of the distributions, the *presence of two peaks*, and the *sensitivity to deflection angle* of the position of the distribution.

The principal features of these distributions can be understood from kinematic considerations. If the gas beam effuses ideally from a thermal source (most probable speed α), if the ground state beam is perfectly collimated, if the detector is small, and if the electron scattering is s-wave, then conservation of momentum and energy determine the following velocity distribution for the metastable atoms in the plane of the incident beams

$$f(v) = \frac{v^2}{V} \frac{v_{0+}^2 \exp(-v_{0+}^2/\alpha^2) + v_{0-}^2 \exp(-v_{0-}^2/\alpha^2)}{[V^2 - \{(m/M)u_0 \sin \Phi - v \sin(\Phi - \theta)\}^2]^{\frac{1}{2}}} \tag{1}$$

for $v_{min} < v < v_{max}$, where

$$v_{\substack{max \\ min}} = \left[\frac{m}{M} u_0 \sin \Phi \pm V\right] \csc(\Phi - \theta) \qquad \begin{cases} \theta < \Phi \\ V < (mu_0/M) \sin \Phi \end{cases} \tag{2}$$

and

$$v_{0\pm} = v \cos(\Phi - \theta) - \frac{m}{M} u_0 \cos \Phi \pm \left\{V^2 - [\frac{m}{M} u_0 \sin \Phi - v \sin(\Phi - \theta)]^2\right\}^{\frac{1}{2}} \tag{3}$$

Here $V = [2m(E - E^*)]^{\frac{1}{2}}/M$; m and M are the masses of the electron and atom respectively; E^* is the energy of the metastable state; and u_0 and E are the speed and kinetic energy, respectively, of the incident electron. The distribution $f(v)$, which is zero outside the limits given in eq. (2), is in disagreement with functions previously presented [7,8]. In the present experiment the detector subtends only a very small angle ($\Delta \theta \approx 0^08'$), but the divergence of the incoming beam ($\Delta \Phi \approx 3^0$) is significant. A numerical integration of eq. (2) over the beam divergence yields curves a of fig. 1.

The present study of velocity distributions in beams of metastable atoms should facilitate the interpretation of experiments such as the fine and hyperfine structure measurements in $2^2S_{\frac{1}{2}}$ hydrogen [1,5], measurements of electron impact excitation of $n = 2$ states in helium [6], time-of-flight studies of repulsive molecular states [7], and analysis of the kinetic properties of single and multi-component gases [8].

References
1. W. E. Lamb Jr. and R. C. Retherford, Phys. Rev. 79 (1950) 549.
2. R. F. Stebbings, W. L. Fite, D. G. Hummer and R. T. Brackmann, Phys. Rev. 119 (1960) 1939.
3. B. Bederson, Atomic Interactions, Part A, eds. B. Bederson and W. L. Fite (Academic Press, Inc., New York, 1968) pp. 89-95.
4. D. P. Donnelly, J. C. Pearl, R. A. Heppner and J. C. Zorn, Rev. Sci. Inst. (to be published). See also pp. 85-87 of ref. 3.
5. J. W. Heberle, H. A. Reich and P. Kusch, Phys. Rev. 101 (1956) 612;
   R. T. Robiscoe, Phys. Rev. 138 (1965) A22 and Phys. Rev. 168 (1968) 4.

6. H. K. Holt and R. V. Krotkov, Phys. Rev. 144 (1966) 82;
   L. Vriens, T. F. M. Bonsen and J. A. Smit, Physica 40 (1968) 229.
7. M. Leventhal, R. T. Robiscoe and K. R. Lea, Phys. Rev. 158 (1967) 49;
   R. Freund and W. Klemperer J. Chem. Phys. 47 (1967) 2897;
   R. Clampitt and A. S. Newton, J. Chem. Phys. 50 (1969) 1997.
8. J. B. French and J. W. Locke in Rarefied gas dynamics, ed. C. L. Brundin (Academic Press, Inc., New York, 1967)
   p. 1461;
   D. A. Crosby and J. C. Zorn, J. Vac. Sci. Tech. 6 (1969) 82.

* * * * *

APPENDIX II

VELOCITY DEPENDENCE OF BEAM ATTENUATION

Consider a monoenergetic beam of atoms (speed v) which
passes a distance ℓ through a Maxwellian gas (density n, most
probable speed α). If the scattering cross section between
an incident particle and a gas particle is σ (here assumed
independent of velocity), then the attenuation of the incident
beam is velocity dependent (Loeb, 1934). The fraction of particles
having speed v which remain in the beam after traveling the
distance ℓ is

$$\exp[-n\sigma\ell\psi(\tfrac{v}{\alpha})]$$

where

$$\psi(x) = \frac{1}{\sqrt{\pi}\, x^2}\left\{x\, \exp[-x^2] + (2x^2+1)\int_0^x dy\, \exp[-y^2]\right\}$$

The function $\psi(x)$ is tabulated in Table A.II.1 and is plotted
in Figure A.II.1.

x	$\psi(x)$
0.05	22.586
0.1	11.321
0.2	5.717
0.3	3.873
0.4	2.969
0.5	2.440
0.6	2.099
0.7	1.863
0.8	1.694
0.9	1.568
1.0	1.472
1.25	1.313
1.5	1.220
1.75	1.163
2.0	1.125
2.5	1.080
3.0	1.056

Table A.II.1 Attenuation Function
$\psi(x)$ vs. x.

The velocity dependent attenuation factor is

$$e^{-n\sigma l \,\Psi(\frac{v}{a})}$$

WHERE

$$\Psi(x) = \frac{1}{\sqrt{\Pi}\,x^2}\left\{x e^{-x^2} + (2x^2 + 1)\int_0^x dy\, e^{-y^2}\right\}$$

$$\Psi(x) \underset{x\to\infty}{\sim} 1 + \frac{1}{2x^2}$$

$$\Psi(x) \underset{x\to 0}{\sim} \frac{2}{\sqrt{\Pi}} \cdot \frac{1}{x}$$
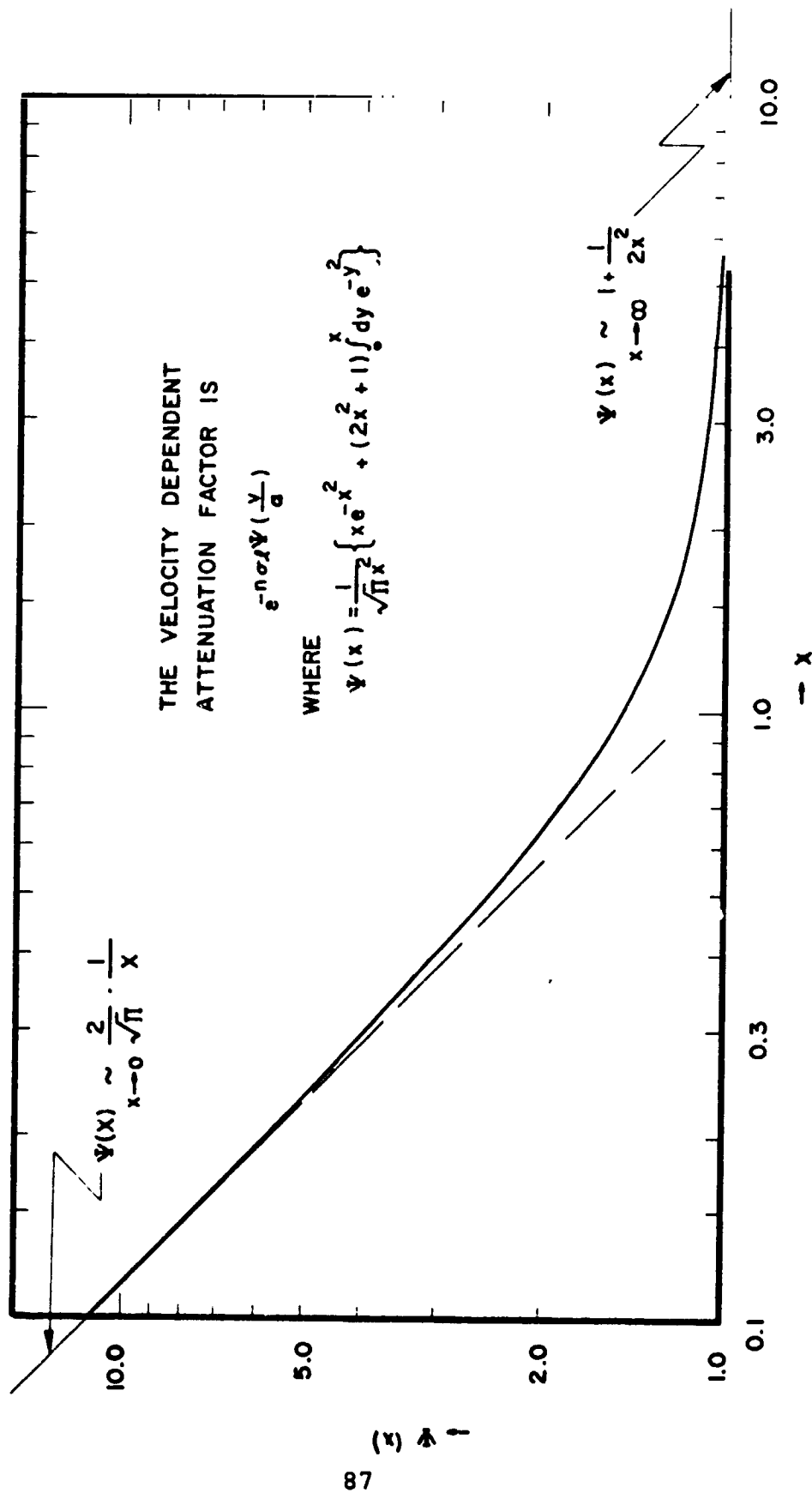
Figure A.II.1 Attenuation Function $\psi(x)$ vs. x

Residual Gas Analysis and Leak Detection by Time of-Flight Measurements on Neutral Metastable Atoms and Molecules*

David A. Crosby† and Jens C. Zorn

Randall Laboratory of Physics, University of Michigan, Ann Arbor. Michigan 84104
(Received 16 August 1968)

We have designed and built a residual gas analyzer which is sensitive to N_2, He, A, Ne, and other molecules which have energetic metastable states. The presence of these gases is revealed by measuring the time of flight of metastable, electrically neutral molecules between a pulsed electron gun and an Auger surface detector. When used as a residual gas analyzer, the present instrument can detect partial pressures of 10^{-7} Torr or greater; when used as a leak detector with helium tracer gas, the instrument can detect leak rates of 10^{-5} Torr liters/sec or larger. The sensitivity of the present instrument can be markedly improved with obvious refinements. The metastable time-of-flight analyzer will operate in a 10^{-4} Torr environment and it has other advantages which may make it a valuable complement to the more conventional methods of leak detection and residual gas analysis.

Introduction

The composition of residual gases in vacuum systems is usually measured by mass spectrometer techniques in which molecules are ionized and then identified by their characteristic charge-to-mass ratio. In this paper, an analyzer is described in which the abundance of certain common gases (H, H_2, He, N_2, CO, A, Ne, and others) is determined by measuring the time of flight of metastable molecules between an excitation region and an Auger surface detector.[1] Compared with the conventional mass spectrometers, the metastable time-of-flight (MTOF) analyzer has the advantages of light weight and ruggedness. The time-of-flight instrument

[1] Metastable time-of-flight methods have been used previously to study molecular beams effusing from *directed* sources. See, for example: J. B. French and J. W. Locke in *Rarefied Gas Dynamics*, C. L. Brundin, Ed. (Academic Press Inc., New York, 1967), p. 1461. R. Freund and W. Klemperer, J. Chem. Phys. **47**, 2897 (1967). J. C. Pearl, D. P. Donnelly, and J. C. Zorn, *International Conference on Atomic Physics Abstracts*, V. W. Cohen and G. zu Putlitz, Eds. (New York University, June 1968), p. 145.

can also be used as a leak detector in several different ways.

The principles of the MTOF analyzer are most easily described by referring to Fig. 1. The molecules within the system are moving in random directions with a Maxwellian distribution of velocities characteristic of the apparatus temperature; further, the pressure is low enough ($<10^{-4}$ Torr) so that the mean free path of gas molecules is at least on the order of the distance between the electron gun and the metastable detector. A short ($\sim10\ \mu$ sec) burst of current is passed through the electron gun and a small fraction of the gas molecules which happen to be in the bombardment region are excited and/or ionized. The ions and electrons are confined by the magnetic field of the electron gun assembly. Most of the excited molecules decay rapidly by emitting radiation, however, many neutral species have metastable excited states and these metastables, along with all the neutral, ground state molecules, will leave the bombardment region with about the same gas kinetic velocity with which they entered. The metastable atoms or molecules can be observed as they arrive at a distant detector several
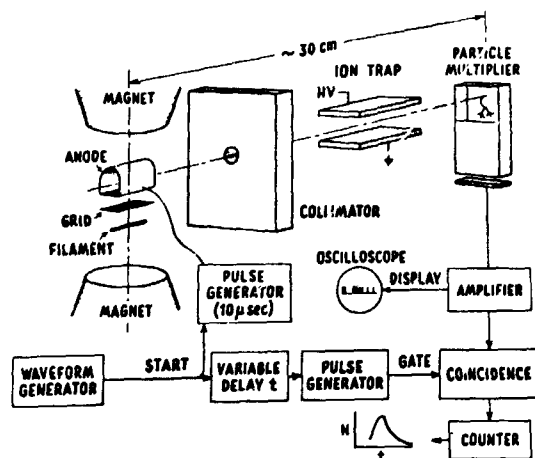
FIGURE 1. Functional block diagram of metastable, time-of-flight analyzer.

hundred microseconds after the end of the electron gun pulse.

Molecules of markedly different mass can be distinguished because their times of flight are proportional to the square root of their masses. Species of comparable mass can often be distinguished by their metastable state energies if the electron energy in the pulsed exciter is well controlled.

I. Apparatus

A. Vacuum System and Gas Control

The experiments described here were done in a brass vacuum envelope, 30 liters in volume, which is maintained at about 1×10^{-7} Torr by a 750-liter/sec oil diffusion pump and a liquid-nitrogen trap. All gaskets are neoprene O-rings.

A fine-control needle valve (Nupro type 2SA) is used to admit gases into the vacuum system. For the measurements described here, the system is maintained at a total pressure between 5×10^{-7} and 5×10^{-4} Torr. For tests of the analyzer's sensitivity to known flow rates of helium, a helium permeation leak (General Electric type #22 HL 020) is used. The conductivity of the leak can be adjusted from zero to 10^{-4} Torr liters/sec by adjusting the leak temperature.

B. Electron Gun

The electron gun provides a current of about 5 mA at an electron energy of 35 eV with an energy resolution of about 2 eV. The directly heated cathode is a 0.003 cm × 0.2 cm tungsten ribbon about 1.5 cm long. The anode potential of the gun is pulsed; a Tektronix model 162 pulse generator is a convenient source for supplying $10-\mu$ sec, 35-V pulses at a rate of 400/sec.

A small permanent magnet (about 800 G) helps to maintain adequate current density within the electron gun.

C. Detector

Metastable species, such as He $(2^3S_1$ or $2^1S_0)$, Ar $(^3P_2$ or $^3P_0)$, and $N_2(a^1\pi_g$ or $A^3 \Sigma_u^+)$, which have excitation energies in excess of a few electron volts can be detected by the Auger ejection of electrons[2] which occurs when the metastables strike a surface. We have found it convenient to use the cathode of a windowless electron multiplier[3] as the Auger surface for our detector: An output pulse from the multiplier then signals the arrival of a metastable atom or molecule. The efficiency of detection is not known, but we estimate that 20% of the metastable helium atoms incident on the multiplier cathode result in an output pulse; the efficiency of the Auger detector for other metastable species is under study. Our experience suggests that the detection efficiency for metastable molecules does not change appreciably even though the Auger detector has often been exposed to air and to backstreaming from unbaffled vacuum pumps.

A pair of metal plates 3 cm long is used to apply an electric field of 100 V/cm transverse to the direction of the metastable beam. This electrostatic trap keeps ions out of the detector and gives a marked improvement in the signal-to-noise ratio at the output of the multiplier.

D. Electronics

The timing and pulse generating requirements of this experiment are met by a Tektronix model 160 waveform generator. The master timer triggers a circuit which supplies the pulse to the anode of the electron gun. A second circuit provides a delayed, $10-\mu$ sec wide pulse to a gate circuit; the gate pulse may be adjusted to occur anytime from zero to 2000 μ sec after the electron gun pulse. The signal pulses from the electron multiplier are amplified and fed to the gate circuit; those signal pulses which arrive during the $10-\mu$ sec open time of the gate are registered on a Hewlett–Packard model 5245 electronic counter.

A multichannel analyzer is now being used to process data from measurements following the ones described here. By using this analyzer in a time-of-flight mode, the entire velocity spectrum can be scanned every time the electron gun is pulsed.

An upper limit to the repetition rate is set by the requirement that molecules excited by the $(n - 1)$th pulse of the electron gun should not affect measurements done during the nth cycle of the apparatus; a rate of 400 Hz is convenient in the present experiment.

II. Results

Figure 2 shows the results found when the system has a 5×10^{-7} Torr partial pressure of helium and a

[2] M. Kaminsky, *Atomic and Ionic Impact Phenomena on Metal Surfaces* (Academic Press Inc., New York, 1965), p. 292.
[3] G. W. Goodrich and W. C. Wiley, Rev. Sci. Instr. **32**, 846 (1961).
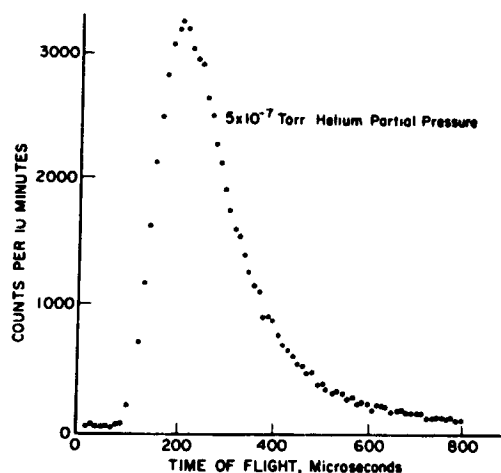
David A. Crosby and Jens C. Zorn

FIGURE 2. Time-of-flight spectrum seen with helium partial pressure of 5×10^{-7} Torr. Total pressure of other detectable species is below 2×10^{-7} Torr.
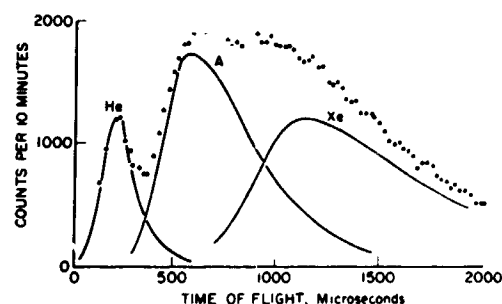

FIGURE 3. Time-of-flight spectrum for a mixture of noble gases: 1×10^{-7} Torr of helium, 1×10^{-7} Torr of argon, and 5×10^{-6} Torr of xenon. The dots show the result from the gas mixture; the solid lines represent what would be found from each of the rate gases separately.

total pressure of other gases less than 1×10^{-7} Torr. The time-of-flight spectrum has the shape that would be expected from a Maxwellian gas at $300°K$. Much smaller partial pressures of helium are detectable; in fact, when the present instrument is used as a leak detector with helium tracer gas, leak rates of 10^{-2} μ liters/sec or larger are easily seen. Obvious refinements should improve this sensitivity.

Figure 3 shows the time-of-flight spectrum obtained when helium, argon, and xenon are all present in the vacuum system. The present instrument can detect partial pressures down to 10^{-7} Torr of those molecules which have energetic metastable states, but we see from the figure that resolution of the heavier species would require additions to the basic time-of-flight method. For example, one possibility would be to correlate the output of the metastable molecule detector with the electron energies in the pulsed exciter.

III. Discussion: Residual Gas Analysis and Leak Detection

Although the cross sections for excitation[4] of the metastable states are on the same order as those for electron impact ionization, the intermittent operation of the electron gun and the lack of spatial focusing put the metastable time-of-flight (MTOF) analyzer at a disadvantage when compared to the usual mass spectrometer. On the other hand, both source and detector in the MTOF system can be very large, so the sensitivity of the present analyzer could probably be much improved.

The MTOF instrument is remarkably resistant to

[4] D. R. Bates, Ed., *Atomic and Molecular Processes* (Academic Press Inc., New York, 1965).

mistreatment. The electron gun cathode is of pure tungsten and requires no special activation; the cathode alignment is not critical so replacement is easy if the filament burns out. The magnetic strip electron multiplier can be exposed to atmosphere for extended periods and still perform effectively; the sensitivity of the instrument does not depend critically on the stability of gain in the multiplier or in amplifier circuits because the pulses are *counted*; moreover the Auger surfaces do not seem to change their efficiency for Helium metastables even after much mistreatment.

The MTOF instrument will operate under very poor vacuum conditions (anything less than 1×10^{-4} Torr is fine; the limit is set by the high-voltage breakdown of the electron multiplier and by the mean free path for the metastables which are to be detected).

The simplicity of the MTOF analyzer makes it feasible to construct its vacuum-housed components as a single unit and leave this attached to the evacuated system. In this way, one set of TOF electronics could serve many installations. Of course, the MTOF analyzer could have its own vacuum pumps and be coupled to the system under test with a throttle valve.

The sensitivity of the MTOF residual gas analyzer to both helium and nitrogen is of particular utility for the detection of leaks in a vacuum system: A high N_2 signal indicates the presence of a leak which can then be pinpointed by using helium as a tracer gas. When the helium actually plays on the leak, the N_2 signal will decrease and the peak of the time-of-flight spectrum will shift to the helium position; if nitrogen and helium signals persist together, it is an indication that still another leak, away from the tracer gas source, exists in the system.

Acknowledgments

90

Detection of Metastable Atoms and Molecules with Continuous Channel Electron Multipliers*

DENIS P. DONNELLY, JOHN C. PEARL, RICHARD A. HEPPNER,
AND JENS C. ZORN

*Randall Laboratory of Physics, The University of Michigan,
Ann Arbor, Michigan 48104*

(Received 14 February 1969; and in final form, 9 May 1969)

BEAMS of metastable molecules can be rapidly and efficiently detected by allowing them to strike the cathode of a windowless electron multiplier. In this note we report on the use of a continuous channel electron multiplier[1] (Bendix "Channeltron") in this application. Compared to other multipliers, the continuous channel multiplier has the advantages of lower noise, simpler circuitry, and far smaller size for a given cathode area.

We have detected thermal beams of metastable helium, hydrogen, neon, argon, krypton, xenon, and molecular nitrogen in our experiments. Although we have not measured the yield of Auger electrons per metastable incident on the multiplier cathode, we judge that the yield is comparable to that achieved[2] on the tungsten or platinum surfaces used in the conventional Auger detectors. The detection efficiency for a given metastable species seems to remain within 10% or so of an equilibrium value in spite of the frequent exposure of the multiplier to humid air and backstreaming pump vapors.

The usual background signal, or dark current, in the Channeltron multiplier is 0.1 counts/sec or less, so it is feasible to do experiments with beam signals as low as 1 count/sec. To maintain a low background count rate it is essential to keep uv radiation (as from bare filaments) and ions (as from vacuum gauge tubes) out of the multiplier. Windows in the vacuum system need not be covered during the experiments, however, since the multiplier does not respond to visible light.

The arrangement shown in Fig. 1 is a simple, effective way to couple the output of the Channeltron to a remote pulse height analyzer.

Sometimes the Channeltrons will develop erratic gain or a very high noise level. This can come from mistreatment such as overloading due to high counting rates or from causes which are less obvious. We have usually found it possible to restore a multiplier to good operating condition by flushing it with acetone or ethyl alcohol and letting it rest on the shelf for a few days. In fact, one of our Channeltrons has been resuscitated in this manner after it had failed from a corona discharge that occurred when the system vacuum was lost with 2.5 kV still applied to the multiplier. A noisy or inoperative multiplier should not be discarded before a few of these "home remedies" have been tried.

The continuous channel multipliers are made of glass tubing which can be broken if too much strain is exerted by the mount; once the multiplier is in place, however,
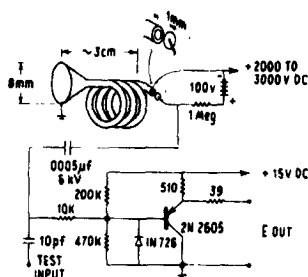

FIG. 1. The Channeltron output is picked up by a small metal button and fed to the input of an emitter follower which is mounted together with the multiplier inside the vacuum chamber. The circuit serves as an impedance transformer so that the signal pulses can be brought out through long, low impedance leads.

the assembly of multiplier plus amplifier on a single board is not overly delicate. It is useful to know that pieces of a broken Channeltron can sometimes still be used for electron multiplication, albeit with lower gain, if new electrical connections for the dc voltage are made to the resistive glass tube with conducting paint.

We are grateful to John Carrico, Christopher Tosswill, Charles Hendee, Barry Kletke, and James Svenson of the Bendix Research Laboratories for the loan of several Channeltron multipliers and for suggestions concerning their use. We thank David Crosby for his contributions to this research.

[1] M. Kaminsky, *Atomic and Ionic Impact Phenomena on Metal Surfaces* (Academic Press Inc., New York, 1965), pp. 292 ff.
[2] G. W. Goodrich and W. C. Wiley, Rev. Sci. Instrum. 33, 761 (1962); D. S. Evans, ibid. 36, 375 (1965).

REFERENCES

Bingham, R. A., "A Stable Aluminum Electron Multiplier,"
    J. Sci. Inst., 43, No. 1, 74-75, January 1966. This
    reference provides construction details for a multi-
    plier of the above type; such details are also avail-
    able from various manufacturers.

Cone, D. R., "Analytical and Developmental Investigation
    of Electron Strip Multipliers, Final Report - Phase
    III" Stanford Research Institute, Menlo Park, California,
    Dec. 1967 (N68-17831).

Crosby, D. A., and Zorn, J. C., "Residual Gas Analysis and
    Leak Detection by Time-of-Flight Measurements on
    Neutral Metastable Atoms and Molecules," J. Vac. Sci.
    Tech., 6, No. 1, 82-84, 1969. Reproduced as Appendix
    III of this report.

Donnelly, D. P., Pearl, J. C., and Zorn, J. C., "Interac-
    tion of Metastable Molecules with Surfaces," in Rare-
    fied Gas Dynamics, H. Wachman and L. Trilling, eds;
    Academic Press, Inc., New York, 1319-1323, 1969a.

Donnelly, D. P., Pearl, J. C., Heppner, R. A., and Zorn,
    J. C., "Detection of Metastable Atoms and Molecules
    with Continuous Channel Electron Multipliers," RSI,
    40, No. 9, 1174, 1969b. Reproduced as Appendix IV
    of this report.

Ehrhardt, H., Langhans, L., and Linder, F., "The Differ-
    ential Excitation Functions of the n = 2 States of
    Helium," Z. Physik, 214, 179-194, 1968. (In German)

Ehrhardt, H., and Willmann, K., "The Angular Dependence of
    the Inelastic Resonance Scattering of Low Energy
    Electrons by Helium," Z. Physik, 203, 1-7, 1967.
    (In German)

Evans, D. S., "Low Energy Charged-Particle Detection
    Using the Continuous Channel Electron Multiplier,"
    RSI, 36, No. 3, 375-382, March 1965.

Frank, L. A., Henderson, N. K., and Swisher, R. L., "Degra-
    dation of Continuous-Channel Electron Multipliers in
    a Laboratory Operating Environment," RSI, 40, No. 5,
    685-689, May 1969.

Freund, R. S., "Molecular-Beam Measurements of the Emission
    Spectrum and Radiative Lifetime of N_2 in the Metastable
    E $^3\Sigma_g^+$ State," J. Chem. Phys., 50, No. 9, 3734-3740,
    May 1, 1969a.

REFERENCES (Continued)

Freund, R. S., "Electron Impact Excitation Functions for
    Metastable States of N_2," J. Chem. Phys., 51, No. 5,
    1979-1982, September 1, 1969b.

Freund, R. S., and Klemperer, N., "Molecular Beam Time-of-
    Flight Measurements for the Study of Metastable and
    Repulsive Electronic States," J. Chem. Phys., 47,
    No. 8, 2897-2904, October 15, 1967.

Goodrich. G. W., Theodorou, D. G., and Lanich, W. A.,
    "Optical Detectors Using Bendix Channeltron[R] Multi-
    pliers," in Proceedings of NAE Conference, May 15,
    1967, unpublished.

Goodrich, G. W., and Wiley, W. C., "Resistance Strip Mag-
    netic Electron Multiplier," RSI, 32, No. 7, 846-849,
    July 1961.

Goodrich. G. W., and Wiley, W. C., "Continuous Channel
    Electron Multiplier," RSI, 33, No. 7, 761-762, July
    1962.

Hagstrum, H. D., "Detection of Metastable Atoms and Ions,"
    J. Appl. Phys., 31, 897, 1960.

Kaminsky, M., Atomic and Ionic Impact Phenomena on Metal
    Surfaces, Academic Press, Inc., New York, 292ff, 1965.

Kirstein, P. T., King, G. S., and Waters, W. E., Space
    Charge Flow, McGraw-Hill, New York, 1967.

Lichten, W., "Lifetime Measurements of Metastable States
    in Molecular Nitrogen," J. Chem. Phys., 26, No. 2,
    306-313, February 1957.

Lichten, W., "New Metastable State of Mercury," Phys. Rev.,
    109, No. 4, 1191-1192, February 15, 1958.

Loeb, L., The Kinetic Theory of Gases, McGraw-Hill, New
    York, 99-103, 1934.

Lurio, A., "Hyperfine Structure of the ^3P States of Zn^{67}
    and Mg^{25}," Phys. Rev., 126, No. 5, 1768-1773, 1 June
    1962.

Marmet, P., and Kerwin, L., "An Improved Electrostatic
    Electron Selector," Can. J. Phys., 38, No. 6, 787-796,
    June 1960.

REFERENCES (Concluded)

McCullough, E. C., "A Detailed Study of Those Factors
    Affecting the Useful Lifetime of the Continuous Channel
    Electron Multiplier, "Nucl. Inst. and Meth., 60, 315-
    353, 1968.

Muschlitz, E. E., Jr., "Metastable Atoms and Molecules,"
    Science, 159, 599-604, February 9, 1968.

Pearl, J. C., Donnelly, D. P. and Zorn, J. C., "Effect of
    Recoil on the Velocity Distribution of Metastable Atoms
    Produced by Electron Impact," Physics Letters, 30A, No.3,
    145-147, October 6, 1969. Reproduced as Appendix I
    of this report.

Pichlik, R., and Zorn, J. C., "A 'Spot-Metering' Residual Gas
    Analyzer," to be published in J. Vac. Sci. Tech., 1970.

Prince, R. H., "The Interaction of Low-Energy Atmospheric
    Ions with Controlled Surfaces," University of Toronto
    Aerospace Institute, UTIAS Report No. 133, 1968 (AD-682 373).

Shyn, T. W., Williams, W. L., Robiscoe, R. T., and Rebane,
    T., "Experimental Value of $\Delta E_H - S_H$ in Hydrogen,"
    Phys. Rev. Lett., 22, No. 24, 1273-1275, June 16, 1969.

Smith, D. G., "Gain Variations in Some Channel Multipliers,"
    J. Sci. Instrum., 43, No. 1, 270-271, April 1966.

Warnock, T. T., and Bernstein, R. B., "Transformation Rela-
    tionships from Center-of-Mass Cross Section and Exci-
    tation Functions to Observable Angular and Velocity
    Distributions of Scattered Flux, "J. Chem. Phys., 49,
    No. 4, 1878-1886, August 15, 1968.

Zorn, J. C., and Pearl, J. C., "A Feasible Satellite Exper-
    iment for Gas Molecule - Solid Surface Interaction
    Studies," University of Michigan, College of Engineering,
    Department of Electrical Engineering, Final Report 08700-
    1-F, October 1967 (N68-10 905).